The Annual Cycle of the Benguela Jet

By

Blessing K. Kamwi

Supervised By

Dr. Jennifer Veitch

Dr. Juliet Hermes

Dr. Marjolaine Krug

Minor dissertation
Submitted in partial fulfilment of the requirement for the degree of Master of Science in Applied Marine Science

Department of Biological Sciences

Faculty of Sciences

University of Cape Town

February 2014

UNIVERSITY OF CAPE TOWN
IYUNIVESITHI YASEKAPA • UNIVERSITEIT VAN KAAPSTAD

PLAGIARISM DECLARATION

1. I know that plagiarism is wrong. Plagiarism is using another's work and to pretend that it is one's own.
2. I have used the Harvard Style reference as the convention for citation and referencing. Each significant contribution to, and quotation in, this thesis/paper from the work, or works of other people has been attributed and has cited and referenced.
3. This thesis/paper is my own work.
4. I have not allowed, and will not allow, anyone to copy my work with the intention of passing it off as his or her own work.
5. I acknowledge that copying someone else's assignment or essay, or part of it, is wrong, and declare that this is my own work.

SIGNATURE: _____

DATE: _____

Table of Contents

Acknowledgements

I would like to send my sincere gratitude to several persons who have been important to the completion of this research project. Many thanks must go to my supervisors: Dr. Juliet Hermes, Dr. Marjolaine Krug and Dr. Jennifer Veitch for the support, knowledge, guidance, encouragement and assistance in data processing throughout the project. Thanks to Dr. Marjolaine Krug for assisting me with the satellite altimetry data. I would also like to thank a number of people that helped in many ways: Bjorn Backeberg, Charine Collins, Yonss Jose, Issufo Halo, Nicolas Barrier, F. Dufois, Professor Frank Shillington, Jasmin Ramershoven, Pavs Pillay and Nadia Jabaar. Special thanks to my family for their support and motivation during my studies.

Lastly I would like to acknowledgement DAAD for the scholarship, Marine Research Institute (Ma-Re) and South African Environmental Observation Network (SAEON) for the partial funding.

Dedication

This research project is dedicated to my parents my mother Josephine Mutenda, my father John Kamwi and my four siblings Namasiku Kamwi, Chosen Kamwi, Abigal Kamwi and Silumbu Kamwi, for the love and encouragement they showed me throughout the project.

Thanks be to God for the wisdom, encourage and strength he gave me, glory be to God.

Abstract

The Benguela Jet is a north-westward flowing current in the southern Benguela region. It is known to have an important influence on the fish recruitment yet little is known about the physical properties of the jet. In this study the ability of satellite data (SST and altimetry) to resolve the Jet was investigated. Following this, the annual cycle of the Benguela Jet was investigated using monthly climatological means computed from both remotely sensed and model output data (from the Regional Ocean Modelling System). Two altimeter tracks were identified as best suited to study the Benguela Jet: the Topex-A / Jason-1A Track number 209 which crosses the Benguela Jet current in its northern region off the Cape Columbine and the Topex-B / Jason-1B track number 31, which crosses the Benguela Jet current in the southern region. The month of January and July were chosen due to the fact that they represent the peaks of summer and winter. The surface geostrophic currents derived from both the model and satellite data reproduced the existence of the jet current off Cape Columbine and the Cape Peninsula. The jet was narrow and strong in January off Cape Columbine and off the Cape Peninsula and was situated farther offshore based on the model, relative to the altimeter data. Outputs from the numerical model showed that in July the jet was confined to the coast and was stronger off the Cape Peninsula (0.5 $m.s^{-1}$) compared to Cape Columbine (0.4 $m.s^{-1}$). A comparison between the regions of strong velocity gradient and the position of the upwelling front were in agreement in depicting the position of the jet. Altimetry, which suffers from limitation in coastal regions, could not reveal the jet in July due to its proximity to the shore at this season. The offshore boundary of the jet is resolved by altimetry in January. The interannual variability of the Benguela Jet has been identified.

Chapter 1: Literature Review

Shelf edge jet currents associated with upwelling have been identified in the world's highly productive eastern boundary upwelling ecosystems. In the southern Benguela upwelling ecosystem a northward flowing Benguela Jet has been documented (Bang & Andrews, 1974). In this chapter, an overview of the dynamics of upwelling systems jet currents is provided. The review provided here also highlights some of the research previously conducted on the Benguela Jet, as well as existing gaps in our knowledge of the jet's dynamics.

1.1 An overview of Jet Currents

Jet currents are a common feature in upwelling systems and are associated with thermal fronts. Upwelling jets occur along density fronts between cold upwelled water and oceanic warm water (Peliz *et al*., 2002). During strong upwelling seasons the fronts are forced farther offshore along with the jets due to persistent upwelling favourable winds (Strub & James, 1995). While during weaker upwelling seasons the fronts and jets are closer to the coast (Strub & James, 1995). These equatorward jet currents have been observed in the world's eastern boundary current regions of California (Barth *et al*., 2000), Chile (Mesias *et al*., 2001), Iberia (Peliz *et al*., 2002) and the southern Benguela (Nelson & Hutchings, 1983).

In the California Current System an equatorward jet current associated with a front off Cape Blanco, Oregon was observed using hydrographic and shipboard Acoustic Doppler Current Profile (ADCP) data (Barth & Smith, 1998). The jet was also observed by Strub *et al*., (1998), using Geosat altimeter and SST data from the Advanced Very High Resolution Radiometer (AVHRR). The finding depicted that the jet occurs along the SST front between warm waters and cooler upwelled waters (Strub *et al*., 1998). The jet tends to be closer to the coast north of Cape Blanco and shifts farther offshore south of Cape Blanco with velocities of 0.5-0.8 $m.s^{-1}$ and a width of 20-50 km (Barth *et al*., 2000). The position of this equatorward jet is within the 200 m isobaths and extends down the water column to approximately 100 m (Barth *et al*., 2005). South of Cape Blanco the jet is located 100 km offshore (Barth *et al*., 2000). The equatorward jet moves offshore in spring/summer (June-August) and close to the coast in winter (December-February) (Strub & James, 2000).

A similar equatorward jet current is also documented as a feature of the Iberian Upwelling System (Amber, 1994). Peliz *et al*., (2002), using hydrographic measurements identified the

jet and recorded a maximum velocity of 0.4 $m.s^{-1}$. When the jet shifts offshore it broadens and has a velocity of 0.25 $m.s^{-1}$ south of Aveiro Lagoon (Peliz *et al*., 2002). The equatorward jet current extends to a depth of approximately 130 m (Peliz *et al*., 2002) and flows over 100-300 m isobaths (Sánchez & Relvas, 2003) with a width of 40 km (Relvas & Barton, 2005).

In the Peru-Chilean System an equatorward jet was identified extending from north to south of Punta Lavapie along the Chilean coast (Mesias *et al*., 2001). North of Punta Lavapie cape the jet meanders offshore (Mesias *et al*., 2003). Mesias *et al*., (2001) used the Princeton Ocean Model (POM) to show that that during peak upwelling south of Punta Lavapie cape, the equatorward jet intensifies reaching 0.4 $m.s^{-1}$ with a width of 50-80 km and extending down to 100 m depth. Whereas north of Punta Lavapie cape the jet current reaches speed of 0.5 $m.s^{-1}$ and extends down to 200 m (Mesias *et al*., 2001).

1.2 Forcing of upwelling jets

Eastern boundary current systems are driven by equatorward, upwelling favourable winds which cause upwelling of cold water and influence the formation of fronts and jets. Equatorward jet currents are related to upwelling dynamics. Studies on upwelling jets around the world have shown that jets are predominantly forced by seasonally varying wind stress (Barth *et al*., 2000; Strub *et al*., 1998; Peliz *et al*., 2002; Mesias *et al*., 2001). The wind stress results in the net offshore transport of warm water, upwelled cold water along the coast and the development of coastal jets that are in geostrophic balance with upwelling isopycnals (Barth *et al*., 2000).

Since upwelling jets are related to the upwelling dynamics these jets are also influenced by the upwelling-favourable wind stress. During upwelling the sea level along the coast is lowered due to wind stress which results in the formation of upwelling fronts and equatorward jets (Mesias *et al*., 2001). In the California Current System an equatorward jet associated with the upwelling front of Cape Blanco was shown to move closer to the coast during upwelling-favourable wind relaxation (Strub & James, 1995). While in summer, intense upwelling favourable wind results in the shift of the jet farther offshore (Barth & Smith, 1998; Barth *et al*., 2005).

Although winds play an important role in the dynamics of upwelling jets, the topography also tends to have a significant influence on the upwelling jets. In the central Chile, the bottom

topography controls the flow of the equatorward jet causing it to separate from the coast off Punta Lavapie (Mesias *et al*., 2003). The offshore movement and decrease in velocity of the Iberian upwelling coastal jet is also due to the influence of the Aveiro Filament (Peliz *et al*., 2002). While the Peru-Chile Trench causes a decrease in the intensity of the equatorward jet (Mesias *et al*., 2003).

The meridional alongshore density gradients also play a role in driving the upwelling jet during weak coastal upwelling in the Iberian system (Peliz *et al*., 2002). Huyer *et al*., (1991), noted that the equatorward jet off northern California is consistent with the thermal wind relation, such that offshore of the jet there is a deepening of the isopycnal and SST isothermal. Whereas inshore the isopycnal and the SST isothermal appears close to sea surface due to coastal upwelling of cold waters (Huyer *et al*., 1991).

The focus of this work is the Bengulea Jet in the southern Benguela region; the following section gives an overview of the region before discussing current knowledge of the Benguela Jet.

1.3 The southern Benguela region

The southern Benguela region extends from 27^{o}S to 35^{o}S along the west coast off Southern Africa (Hardman-Mountford *et al*., 2003). This region is separated from the northern Benguela region by an intense permanent upwelling cell off Lüderitz along the Namibian coast where strong winds and offshore transport provide a barrier to pelagic fish species (Hardman-Mountford *et al*., 2003).

The southern Benguela consists of the West Coast and Western Agulhas Bank (Pitcher *et al*., 2008). The West Coast is characterized by coastal upwelling associated with intense upwelling cells such as the Cape Peninsula, Cape Columbine and Namaqua cells (Weeks *et al*., 2006) and provides nursery ground for pelagic fisheries (van der Lingen & Huggett, 2003). These cells have been associated with a maximum in wind stress curl (Shannon & Nelson, 1996). The West Coast is highly productive as compared to the western Agulhas Bank. The western Agulhas Bank has a broader shelf from 18-26^{o}E and forms the southern boundary of the Benguela ecosystem (Blanke *et al*., 2009). This area is also a major spawning ground for the pelagic fishery and is characterised by strong vertical stratification of the water column in summer and highly mixed in winter (McMurray *et al*., 1992).

The Benguela Jet is situated on the shelf in the southern Benguela, where surface currents are predominantly equatorward (Figure 1.1) (Hardman-Mountford *et al.*, 2003; Shannon & Nelson, 1996). The jet current plays an essential role in linking and transporting ichthyoplankton from the spawning grounds of the Agulhas Bank to the nursery grounds of the west coast which are approximately 500 km apart (Hutchings & Boyd, 1992; van der Lingen & Huggett, 2003). This region is also influenced by the warm water of the Agulhas Current, which enters the Benguela around the southern tip of Africa in the form of large Agulhas eddies, rings or filaments (Veitch, 2009). The influx of the Agulhas water has an influence on the dynamics of the southern Benguela, interacting with the upwelling frontal system and linking the Benguela Current to the Indian Ocean (Blanke *et al.*, 2009). The interaction of the upwelled water and the Agulhas water is unique as no other eastern boundary current system has a similar process (Shillington *et al.*, 2006). The coastal upwelling and the warm Agulhas Current, as well as the Benguela Jet, are the main oceanographic features dominating and influencing the biology in the region (van der Lingen & Huggett, 2003).

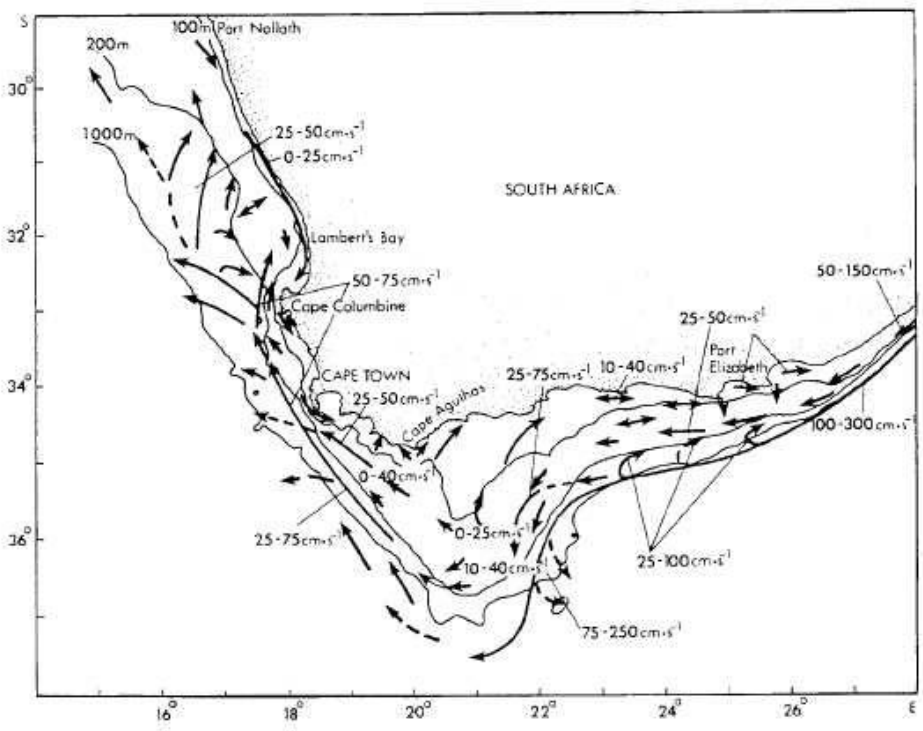

Figure 1.1. *Schematic of surface currents estimated from ADCP data retrieved between November and January 1992. Vectors represent estimated typical velocity values in the southern Benguela region (From Boyd et al., 1992).*

1.4 Atmospheric forcing of the southern Benguela

The southern Benguela is influenced by the South Atlantic Anticyclone (SAA) and continental heat low (Shillington, 1998). The SAA has a seasonal movement of southward (northward) in austral summer (winter), facilitating the seasonal variability of the upwelling favourable wind (Preston-Whyte & Tyson, 1993). When the SAA moves southward, it induces upwelling favourable south-easterly winds in the southern Benguela (Shillington, 1998). However northward shifts and weakening of the low pressure trough results in the weakening of the upwelling favourable winds and dominance of northwesterly winds, which are favourable conditions for downwelling (Shillington, 1998).

During late austral spring (September-November) and summer (December-February) intense south-easterly wind results in dominantly northward flowing currents (Huggett *et al.*, 1998). The surface currents in the southern Benguela respond to variation in the direction and magnitude of the wind forcing (Fawcett, Pitcher & Shillington, 2008). A low-level atmospheric jet along the west coast in the Benguela region has been documented by Nicholson (2009). This low-level atmospheric jet forms due to the thermal difference

between the land and ocean (Nicholson, 2010). The atmospheric jet blows parallel to the coast and enhances coastal upwelling (Nicholson, 2010). The upwelling intensity corresponds to the intensity of the low-level atmospheric jet, which intensifies during spring (Nicholson, 2010).

1.5 The Benguela Jet current

The northward flowing Benguela Jet current was first described by Bang and Andrews (1974) using current meters. They noted the position and character associated with the gradient between warm oceanic waters and the cool, coastal upwelled water. The water of the Benguela Jet consists of western Agulhas Bank waters and Agulhas Current water which leak into the west coast shelf-edge (Boyd & Nelson, 1998). An uplift of the isopycnals at the shelf edge creates this northward flowing jet current off the Cape Peninsula and Cape Columbine (Nelson, 1989). Nelson (1989) showed the jet to be strongest near Cape Columbine where topography is steepest, with a typical speed of 0.5 $m.s^{-1}$. Strub *et al*., (1998), noted that the jet current is strengthened by the Agulhas water with high steric height. Using Acoustic Doppler Current Profiler (ADCP) observations Boyd and Nelson (1998) estimated the speed of the jet to range from 0.4 $m.s^{-1}$ to 0.8 $m.s^{-1}$. The jet current separates into offshore and shoreward components near Cape Columbine (Boyd *et al*., 1992). The Benguela Jet current is characterised by a width of 20-30 km and varies between the 200 and 500 m isobaths (van der Lingen & Huggett, 2003). Butler (2012), using ADCP and CTD data noted the jet extending to about 300m depth in summer and to about 120 m depth in winter.

1.5.1 Forcing of the Benguela Jet

In order to understand the dynamics of the jet, it is important to note the possible forcing of such a feature. According to Bang and Andrews (1974), the existence of the jet is related to a strong thermal front between warmer oceanic water and upwelled cold water. Strub *et al*., (1998) noted that during spring and summer the SST gradient is intense and closest to the coast. The position of the thermal upwelling front is coincident with regions of high SSH gradient (Lutjeharms, 1981). The thermal front also influences the location of the jet; the thermal front is stronger in summer due to intense coastal upwelling and weaker in winter as upwelling is weaker (van der Lingen & Huggett, 2003).

The occurrence of the Benguela Jet along the SST frontal gradient is similar to other equatorward jet currents found in the Iberian and Californian systems (Peliz *et al*., 2002; Barth *et al*., 2000). The Benguela Jet differs from other equatorward jet currents because it is enhanced and maintained by the influx of low density Agulhas water (Bang & Andrews, 1974) on its seaward boundary. Strub *et al.,* (1998), using satellite measurements of SSH and SST, found that the inflow of warm and low density water from the Agulhas Current into the Benguela act to maintain and enhance the thermal and pressure front which drive the Benguela Jet.

Like other upwelling jets the Benguela Jet is also influenced by the wind stress that drives upwelling in the southern Benguela (Bakun & Nelson, 1991). The equatorward wind stress results in the formation of an upwelling front and an equatorward jet (Boyd & Nelson, 1998). The intensity of the current is predominantly associated with the wind stress (e.g. Bang & Andrews, 1974; Boyd & Nelson, 1998). Figure 1.2 and1.3 shows the wind stress curl and surface wind stress over a period of 12 months. The wind stress curl and surface wind stress both intensify in spring (September-November) and summer (December-February) and weaken in autumn (March-May) and winter (June-August) months which relates to the strengthening and weakening of the jet in the southern Benguela (Bakun & Nelson, 1991). The position and character of the current are associated with the wind-driven coastal upwelling (Bang & Andrews, 1974). The transfer of energy from the wind to the ocean is essential for overcoming stronger inshore frictional forces (Bang & Andrews, 1974). The wind energy enhances the formation of the offshore jet and can maintain the jet farther offshore (Bang & Andrews, 1974). However when the energy is less and weaker the jet moves shoreward (Bang & Andrews, 1974). During summer the SST gradient is stronger as the upwelling increases whereas in winter the SST gradient is weaker (van der Lingen and Huggett, 2003).

Veitch (2009) suggests that the upwelling front associated with the jet current is topographically controlled, in such a way that the front follows the shelf-edge. The other possibility of forcing may be due to the jet current being density driven. Upwelling fronts that are induced by the different forcings account for some of the variability in the Benguela Jet current.

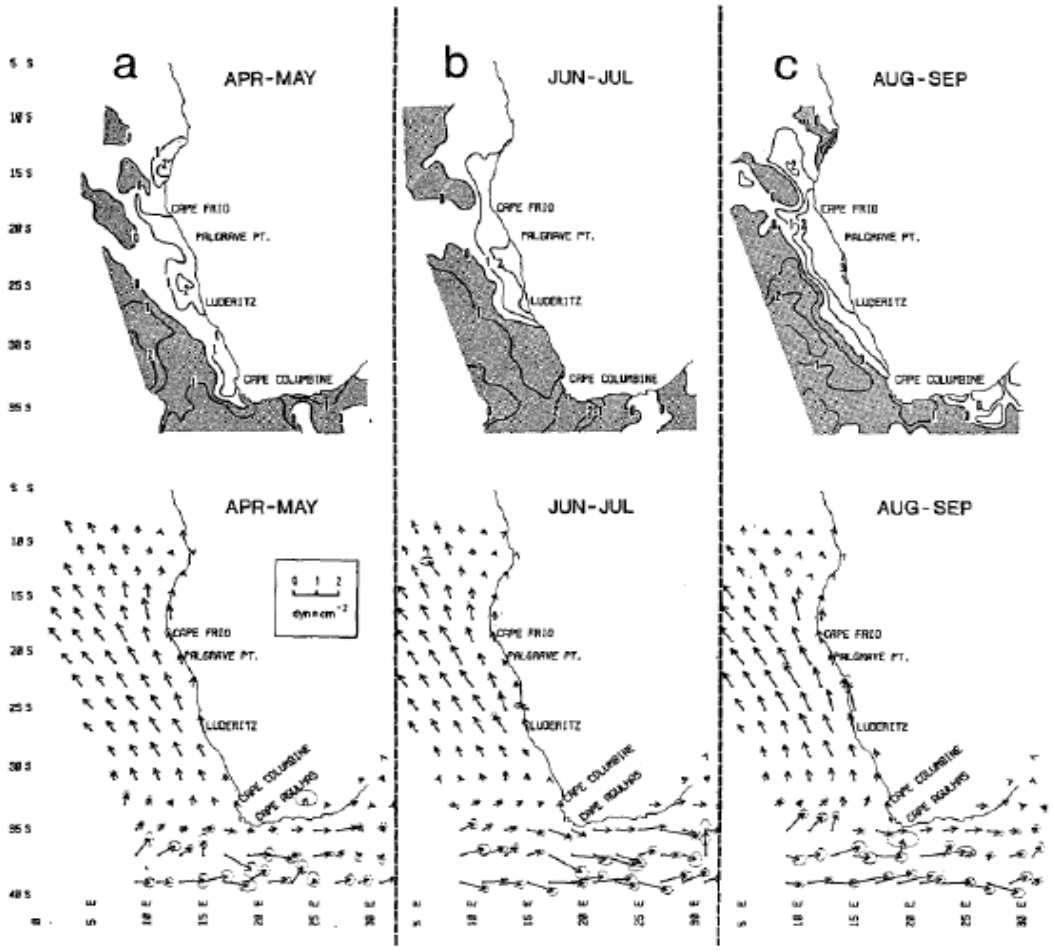

Figure 1.2. *a-c) Schematic of the wind stress curl (top) and surface wind stress (bottom) for April to September in the Benguela system. Shaded areas indicate the areas of anticyclonic wind stress curl. (From Bakun and Nelson, 1991).*

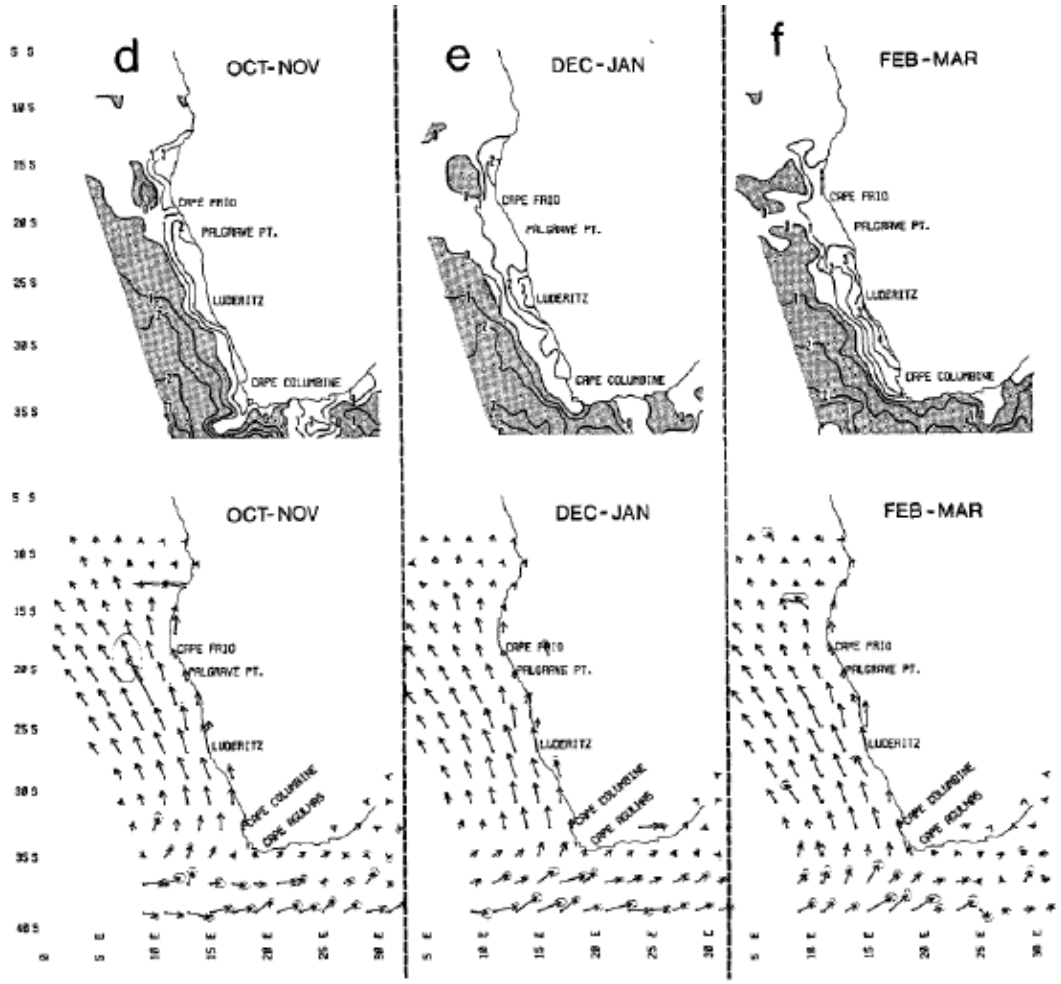

Figure 1.3. *d-f) Schematic of the wind stress curl (top) and surface wind stress (bottom) for April to September in the Benguela system. Shaded areas indicate the areas of anticyclonic wind stress curl. (From Bakun and Nelson, 1991).*

1.5.2 Variability of the Benguela Jet

The Benguela Jet current tends to be situated close to shore during winter, mid-spring and shifts further offshore in summer based on the 1995/1996 season (Huggett *et al*., 1998). The jet has been documented to be a spring and summer feature off the Cape Peninsula (Fowler & Boyd, 1998), which is consistent with the peak upwelling season. Butler (2012), based on ADCP and CTD data observed the position of the jet between 17.6°E-17.9°E offshore in summer and between 17.7°E-18.1°E closer to the coast in winter off Cape Peninsula. Current velocities in the jet can reach 0.5-0.75 $m.s^{-1}$ at the peak of the upwelling season in spring and summer (Boyd *et al*., 1992). From model data, Veitch *et al*., (2009) also found that the current is stronger and narrower in summer as compared to winter when the current is weaker and broader. Veitch *et al.,* (2009) used model output to suggest that the current is present in

both summer and winter off the Cape Peninsula, but extends all the way up to Cape Columbine only in summer. This proposed seasonal variability of the jet correlates to upwelling intensity.

Strub *et al*., (1998) based on Geosat altimeter with two years data measurement of SSH, noted that the jet shifts offshore during autumn and winter. During spring and summer the jet is situated closer to the coast (Strub *et al*., 1998). However Boyd and Nelson (1998), based on ADCP and drogue tracking, suggest that sustained upwelling-favourable wind drives the jet current farther offshore in spring and summer. This seasonal variability of the flow of the jet may have a significant impact on the biology particularly on the pelagic fishery in the southern Benguela.

1.5.3 Biological Significance

The Benguela Jet current has been documented to play a significant role in the recruitment of commercially exploited fish species such as sardine *Sardinops sagax* and anchovy *Engraulis capensis* (van der Lingen & Huggett, 2003). These species spawn in warmer, lower productivity waters of the Western Agulhas Bank, where eggs and early larvae are then transported to the west coast nursery grounds where productivity is high (Figure 2) (Shelton & Hutchings, 1982). The eggs within the jet current hatch and the larvae reach the west coast nursery ground where the larvae enter retention areas and can continue to grow (Mullon *et al*., 2003). In this case, the timing of spawning in relation to the jet current is essential for recruitment success (Hutchings *et al*., 1998). Therefore, there must be a coupling between the two processes (Mullon *et al.,* 2003).

The capacity of the jet current to transport eggs and larvae was first investigated by using a free drifting parachute drogue which was entrained into the jet current displaying the significance of the jet (Shelton & Hutchings, 1982). Boyd *et al*., (1992) using ADCP data, noted the funnelling of anchovy eggs from the western Agulhas Bank to the west coast nursery grounds by the jet. Huggett *et al*., (2003), using a particle tracking model (individual-based model) supported the hypothesis of Shelton and Hutchings (1982), that the jet current transports spawning products of anchovy and sardine to the west coast nursery areas. The jet current also transports eggs and larvae for Cape hake *Merluccius spp* (Grote *et al.,* 2007). The stability in anchovy recruitment can be attributed to the resilience of the jet current transport and the low north-westerly wind (Shelton and Hutchings, 1982). Larvae transported by the

jet may penetrate the aged upwelled water leading to low starvation mortality and may contribute towards recruitment when the larvae enter the retention region in St Helena Bay (Shelton & Hutchings, 1982). Figure 1.4 below illustrates the biological significance of the current in the Southern Benguela region.

Although the jet current plays a major role in recruitment, offshore divergence of the jet current can also cause loss of small pelagic eggs and early larvae (van der Lingen & Huggett, 2003). However, some of the eggs and larvae could reach the nursery grounds through the onshore current north off Cape Columbine (Fowler & Boyd, 1998).

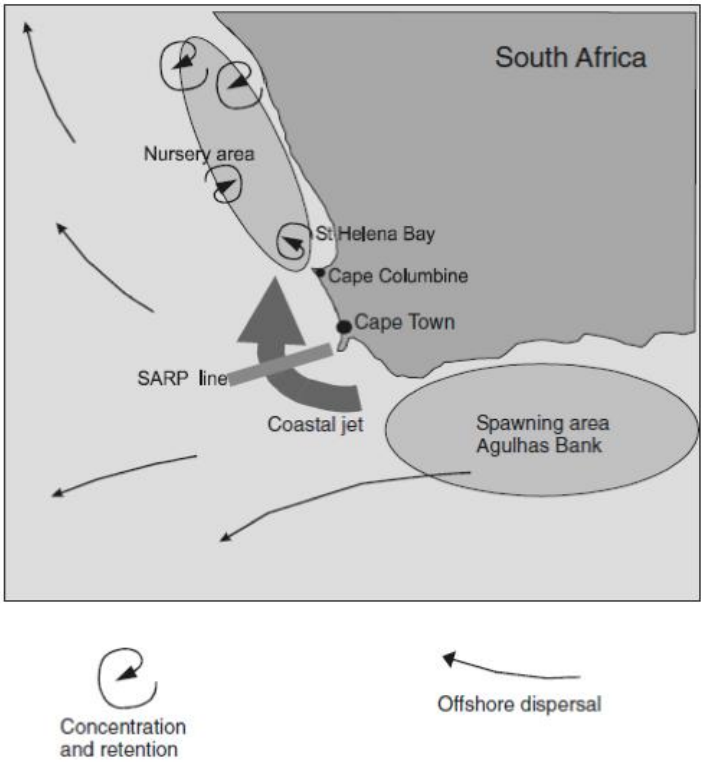

Figure 1.4. *Schematic of the Southern Benguela illustrating the spawning grounds at Agulhas Bank, nursery grounds of the anchovy off St Helena Bay and the coastal jet current and the SARP line across the jet (From Hutchings et al., 1998).*

The South African Anchovy and Sardine Recruitment Programme (SARP) monitoring line was instigated in 1995 with the aim of monitoring and providing information on the temporal transport of ichthyoplankton by the Benguela Jet current (van der Lingen & Huggett, 2003). The monitoring transect crosses the jet current off the Cape Peninsula (Huggett *et al*., 1998) (Figure 1.3). The transect is monitored due to the fact that the jet current is essential in

transporting eggs and larvae which may play an important role in predicting recruitment success (Hutchings, 1992). Through the SARP line, the importance of the jet current as a transport mechanism was identified supporting the hypothesis initially suggested by Shelton and Hutchings (1982).

Chapter 2: Research Findings

2.1 Introduction

The Benguela Jet is an equatorward flowing current that extends to the depths of 300 m between the 200 m and 500 m isobaths in the southern Benguela (van der Lingen & Huggett, 2003; Butler, 2012), with an estimated width of 20-30 km (Nelson & Hutchings, 1983). The Jet current is situated off the Cape regions namely the Cape Peninsula (34^{o}S) and Cape Columbine (33^{o}S) along the west coast of South Africa (Boyd *et al*., 1992) (Figure 2.1).

The Benguela Jet current owes its existence to the presence of a thermal and pressure front which occurs between cold upwelled coastal waters and the warm oceanic waters (van der Lingen & Huggett, 2003). This presence of an upwelling jet at the interface between the upwelled coastal waters and warmer oceanic waters has been documented in other regions of the world such as the Iberian and Californian upwelling systems (Strub *et al*., 1998; Peliz *et al*., 2002). The Benguela Jet is unique compared to other equatorward jet currents because it is enhanced and maintained by the influx of low density Agulhas waters (Bang & Andrews, 1974). The jet is strengthened by the influx of water from the Agulhas Current with high steric heights and cold upwelled water with low steric heights (Strub *et al*., 1998).

Studies on the influence of the Benguela Jet have increased due to the SARP monitoring line (van der Lingen & Huggett, 2003). This research program has focused on the biological importance of the jet; however, little has been done regarding the physics driving the jet. Therefore this study focuses on the physics and dynamics of the Benguela Jet current using remotely sensed sea surface temperature (SST), sea surface height (SSH) and model output data. It is anticipated that the work done in this study will assist both the scientific research programmes and fisheries managers in understanding the mechanisms that influence the Benguela Jet (and hence the sardine and anchovy recruitment).

The role of the jet current as a transport mechanism was first hypothesized by Shelton and Hutchings (1982). The transport of fish eggs and larvae is one of the important environmental processes that influence recruitment (Fowler & Boyd, 1998). Since the spawning and nursery grounds are 500 km apart, understanding the physical dynamics of the Jet current involved in the transport of eggs and larvae is essential in the recruitment and management of fisheries.

The importance of near-surface circulation pattern in terms of influencing the marine biota has formed one of the key basis of investigations in the southern Benguela (Boyd et al., 1992; Shelton & Hutchings, 1982).

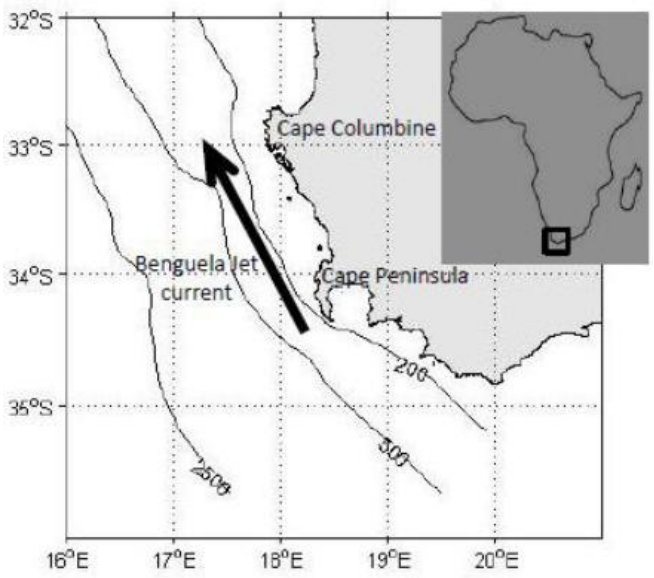

Figure 2.1. *Bathymetry of the Southern Benguela region with the Benguela Jet current off Cape Columbine (33°) and Cape Peninsula (34°). The 200, 500 and 2500 m isobaths are shown.*

This study aims to address the following:

- Can the Jet be identified in altimeter and SST satellite data?
- How well does the jet in the satellite data compare to the model?
- What is the annual cycle of the jet (both position and strength)?

The outline of this paper is as follows: An overview on the work that has been done on the Benguela Jet current is presented in chapter one, including work that has been done on other upwelling jet currents. Chapter two provides a description of the methodology and datasets used in this thesis as well as the findings based on the satellite datasets and model (ROMS) output data. The discussion on the findings is provided in this chapter. Chapter three provides the summary and conclusion of this study.

2.2 Data and Methods

In this study the annual cycle of the Benguela Jet is investigated, using both remotely sensed and model data (from ROMS). Satellite measurements of sea surface height (SSH) and sea surface temperature (SST) are used. The remotely sensed data is used in conjunction with

model data from the Regional Ocean Model System (ROMS), which was previously successfully run over the Benguela region (Veitch, 2009). Satellite remote sensing has enhanced our ability to study and understand the world's oceans through the retrieval of different parameters such as SST and SSH. The satellite data used to study the Benguela Jet current only measures signals at the ocean surface. The model output data is used primarily for comparing the modelled surface properties of the Benguela Jet to the observations from satellite data. A description of the satellite and numerical model datasets used in this study is provided below.

2.2.1 Satellite Datasets

MODIS Sea Surface Temperature

Infra-red sensors have provided routine observations of SST over the world's oceans since the early 1980s (Dufois *et al*., 2012). Today, SST is retrieved from sensors located on both geostationary and polar orbiting satellites (Merchant *et al*., 2009). In this study SST observations are derived from broad-band infrared radiances measured by the MODIS instrument onboard the Terra satellite. Terra satellite MODIS and not Aqua were used as a complete archive of processed data as well as climatology already existed. The Terra climatology is also derived using a longer time-series than Aqua (2 more years). MODIS images the entire earth every 1 to 2 days, using 36 spectral bands with spatial resolutions varying between 200 m, 500 m and 1000 m (Robinson, 2010). SST from MODIS is either derived from the thermal IR (11 and 12 μm) channels or the mid-IR region (3.8 and 4.1 μm) channels (Minnett *et al*., 2002). The MODIS dataset used in this study consists in the 1km daytime MODIS SST processed by Dufois & Rouault (2012) over the period 2000-2009. The daytime data was selected as the time of acquisition is 8:00 AM, where the impact of solar radiation on the SST is minimized and allows the usage of cloud flag CLDICE to remove contaminated pixels near cloud edges (Dufois *et al*., 2012). Daily data download from (http://oceancolor.gsfc.nasa.gov) were averaged to monthly and then to monthly climatology. The monthly SST climatology used in this study was that of Dufois *et al*., (2012).

Altimetry Sea Surface Height

SSH measurements can be related to the ocean's current velocity field through the geostrophic approximation and have been used to study ocean circulation for more than two

decades (Rouault *et al*., 2010). SSH is measured from different altimeter missions such as the Jason and Topex.

Altimeters are active radar sensors providing observations of sea level by measuring the time difference between the transmitted radar pulse and its echo from the ocean's surface (Robinson, 2010). The distance between the satellite and the sea surface, called the altitude, is referenced to a fixed ellipsoid to track variation in time of the SSH (Rouault, 2011). The reference ellipsoid is an approximation of the Earth's surface, while the range is the distance from the satellite to the sea surface (Figure 2.2) (Robinson, 2010). SSH retrieved from altimeters is expressed as follows:

$$\text{SSH} = \text{Altitude} - \text{Range}. \qquad (1.1)$$

Physical factors such as the geoid, tides, sea state and winds contribute to the influence of the SSH measured by altimeters (Rouault, 2011). The schematic in Figure 3 illustrates different factors that contribute to the measurement of SSH by altimeters. Two important measurements from altimetry data of interest to oceanographers are the mean dynamic topography (MDT) and the sea level anomaly (SLA) (Rouault, 2011). The MDT is basically the difference between the mean sea level and the geoid and the SLA is accountable for the current variability after the removal of effects of tides, atmospheric pressure and sea state (Rouault, 2011). The Absolute Dynamic Topography (ADT) is then computed by adding the MDT to the SLA.

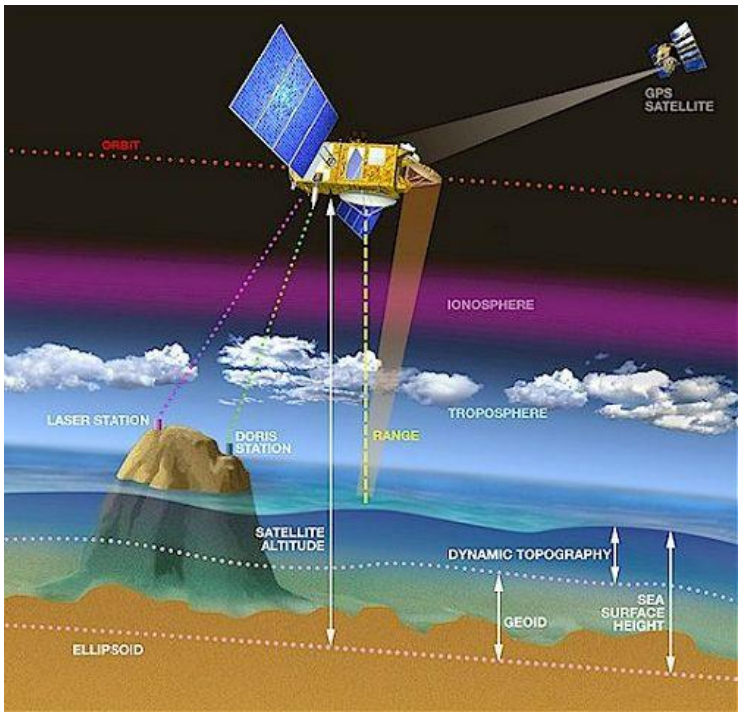

Figure 2.2. *Parameters used for computing the absolute dynamic topography from altimeter (From http://www.altimetry.info/images/alti/principle/methode_en.jpg).*

In this study, SSH observations were extracted along Jason-1 and Topex altimeter tracks. SLA measurements were downloaded from the Radar Altimeter Database System (RADS) website (http://rads.tudelft.nl/rads/rads.shtml). The SLA was processed using the RADS default processing which includes geophysical corrections for the effect of tides, barometric pressure, geoid, sea state, the dry ionosphere and the wet troposphere. The SSH data from the two altimeter missions were used to compute the mean SSH which was then subtracted from the SSH to obtain the SLA, the mean sea surface (MSS) was derived from the OSU MSS95 mean sea surface model (Schrama *et al*., 2000).

From all the altimeter's tracked along which data has been acquired since 1992, two were identified as best suited to study the Benguela Jet: the Topex-A / Jason-1A Track number 209 which crosses the Benguela Jet current in the northern region off the Cape Columbine (Figure 2.3) and the Topex-B / Jason-1B track number 31, which crosses the Benguela Jet current in the southern region (Figure 2.3). It is important to note that only the current flowing perpendicular to the satellite altimeter tracks is reproduced by the derived across geostrophic velocities. Therefore it is vital to find the altimeter track which will capture the stronger

component of the flow. The period of data acquisition for each of the altimeter's mission selected for this study is presented in Table 1.

The CLS09 MDT of Rio and Larnicol (2011) with a $1/4^{o}$ resolution were interpolated to a 0.01 degree resolution and then extracted along the altimeter tracks. The monthly SLA averages were computed from the 10 days interval and averaged to produce a monthly climatology of SLAs. The SLAs were then added to the CLS09 MDT to obtain the ADT monthly climatologies.

In terms of limitation the altimetry data suffer from contamination close to the coast within a 50 km band. This is due to land contamination and difficulties in the wet tropospheric correction which leads to errors in the SSH (Krug & Tournade, 2012). Altimeter data is also limited close to the coast due to difficulties of resolving high frequency signals from tidal and atmospheric forcing (Krug & Tournade, 2012). Another challenge of altimeter data is the estimation of high resolution MDT (Krug & Tournade, 2012), this is due to the lack of high resolution of the geoid.

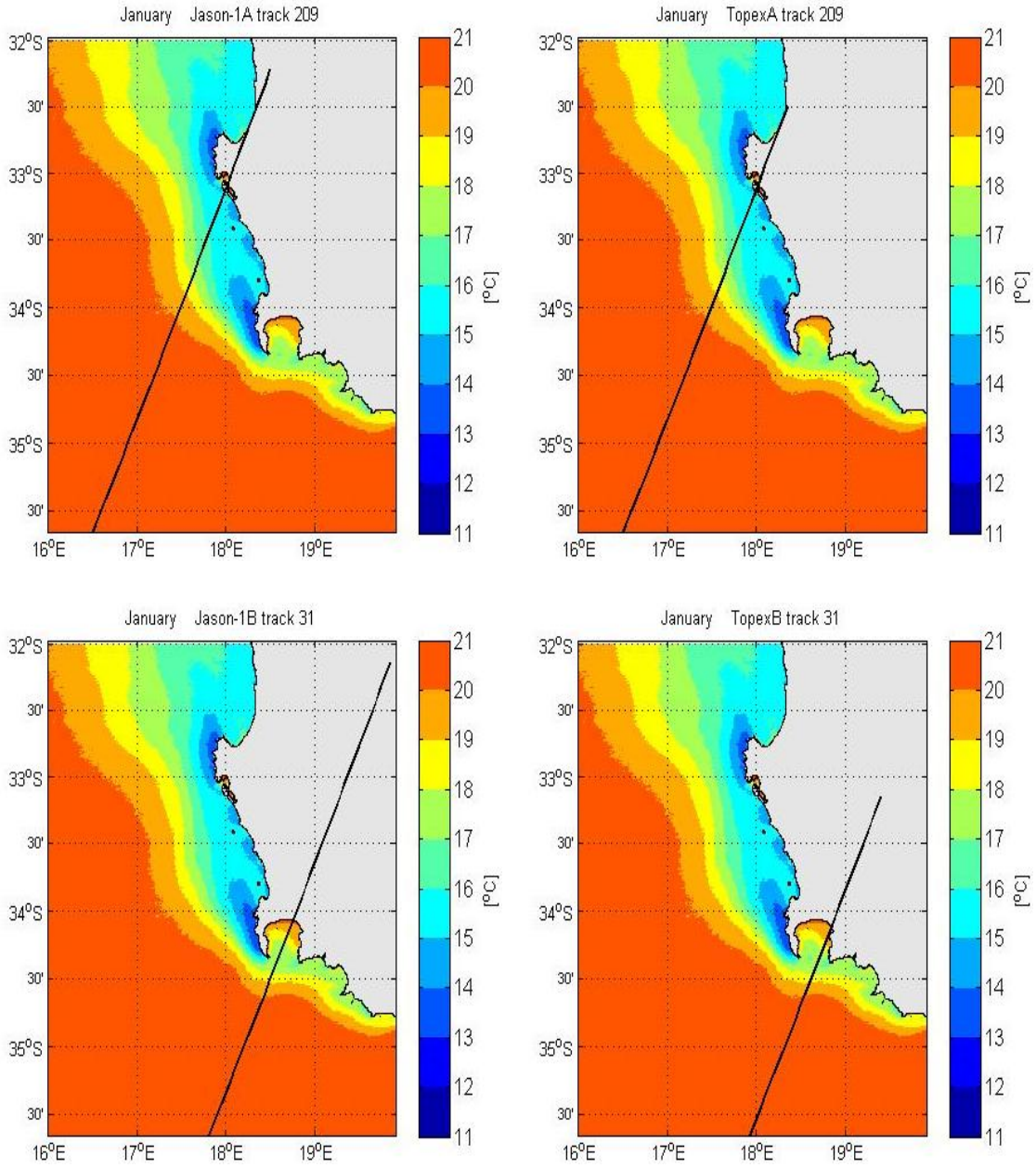

Figure 2.3. *Snapshot of MODIS SST climatology of January and Altimeter tracks lines. Northern tracks: Jason1A and Topex A track 209 (top) and southern tracks Jason1B and TopexB track 31 (bottom). Solid line indicates the tracks from which the data is used to compute geostrophic velocities.*

Table 1: *Jason1 and Topex altimetry missions with each phase and track numbers were available at different time intervals were identified as best suitable to study the Benguela Jet.*

Mission	Phase	Track	Time interval availability
Jason 1	A	209	2002-2009
	B	31	2009-2012
Topex	A	209	1992-2002
	B	31	2002-2005

2.2.2 Model Description.

Model output of monthly climatological SST and SSH were retrieved from the Regional Ocean Model Systems (ROMS) (Veitch, 2009). The model set-up which has been used for this study is that of Veitch (2009), which has a resolution of 9 km. The model solves free-surface primitive equations based on the Boussinesq and hydrostatic assumptions (Penven *et al*., 2001). It incorporates the advection/diffusion equations for potential temperature and salinity as well as for the nonlinear equation of state (Veitch, 2009). Primary variables incorporated into the model are temperature, salinity, surface elevation, barotropic and baroclinic horizontal velocity components (Veitch, 2009). High-order numerics and advanced features integrated into ROMS provide a robust resolution of mesoscale feature of oceanic and coastal regions (Penven, *et al*., 2001). The terrain-following coordinate nature of the model allows resolution enhancement of sea surface or region of interest (Penven, *et al*., 2001). For a complete description of the model formulation the reader is referred to Shchepetkin and McWilliams (2005) and Veitch (2009).

The model has been used to study the Southern Benguela region and has been shown to well represent the key features associated to this region (Veitch *et al*., 2010; Veitch *et al*., 2009; Veitch, 2009). Since this study addresses the annual dynamics of the jet, all the forcing in the model are derived from climatology. The nested configuration of the model was forced with monthly climatology wind data from 0.5^{o} QuikSCAT spanning 2000-2007 (Veitch, 2009). The use of monthly mean climatological wind data removes high-frequency variability of the wind. This results in the persistent equatorward upwelling–favourable wind forcing. The wind forcing plays an important role in driving upwelling along the southern Benguela, which also influence the development of the Benguela Jet.

2.2.3 Methodology

Gradient Analysis

SST and SSH retrieved from satellite were used to compute the gradients along the altimeter tracks with equations (1.2 and 1.3) below. The region of strong SST and SSH gradients are expected to show the position of the front and the jet. The negative gradients indicate the southward flow and the positive gradient indicate the northward flow. The strongest SST and SSH gradients were between the region of 17.4-17.6^{o}E and was thus chosen to represent where the jet usually resides. Six vectors of the satellite-derived surface geostrophic

velocities were calculated within this domain, that were then used to create a climatology from 8 (spanning 2002 to 2009) and 11 (spanning 1992 to 2002) years of data from the Jason1A 209 and TopexA 209 tracks respectively.

$$SSH_{gradient} = \frac{\Delta SSH[m]}{d_{SSH}[m]} \qquad SST_{gradient} = \frac{\Delta SST[°C]}{d_{SST}[m]} \qquad (1.2), (1.3)$$

Where $SSH_{gradient}$ is the SSH gradient and $SST_{gradient}$ is the SST gradient, ΔSSH and ΔSST are the changes in SSH and SST, d_{SSH} and d_{SST} are the distances of SSH and SST data along the altimeter tracks.

Geostrophic velocities

The geostrophic velocities derived from both the numerical model output and the altimeter datasets were computed in the same way for better comparison between the two datasets. The geostrophic current velocities across the altimeter's tracks were computed from the ADT monthly climatologies for each altimetry mission using equation (1.4). The geostrophic velocities were derived from 8 years of data from Jason1A 209 and 11 years from TopexA 209 as well as 4 years of data from both for Jason1A 31 and TopexA 31 altimeter tracks. While the geostrophic current from the model were computed using the model monthly climatologies SSH (ξ) in equation (1.4) with ξ replacing the ADT term in the equation.

$$u_g = -\frac{g}{f}\frac{\partial ADT}{\partial y}$$
$$v_g = \frac{g}{f}\frac{\partial ADT}{\partial x} \qquad (1.4)$$

Where u_g and v_g are the zonal and meridional geostrophic current velocities, g is the gravitational acceleration and *f* is the coriolis parameter, *x* and *y* are the zonal and meridional.

2.3 Results

In this section the ROMS model output and the satellite datasets (as described in Section 2.2), particularly the different missions are used to investigate the dynamics of the jet. The model and satellite altimetry data are then compared with each other. Jason-1A (Topex-A) track 209 will be referred to as J1_209 (Tp_209) and Jason-1B (Topex-B) track 031 as J1_31 (Tp_31). January and July months are chosen to highlight typical austral summer and winter

flow patterns. These results are based on climatology calculated from the model and the satellite data (as described in Section 2).

2.3.1 Benguela Jet current based on model output data

The ROMS configuration used here was forced with monthly climatological wind data from 0.5^{o} QuikSCAT spanning 2000-2007 (more details in Section 2.2 in this Chapter). The model with, a high resolution of 9 km, should accurately resolve the Benguela Jet. The geostrophic currents were calculated from the model output derived SSH as described (in Section 2.2). The difference between total surface current and geostrophic current is that the total surface currents are obtained from the u and v components which are the surface ocean current variables. The total surface current represents the overall flow estimated from the numerical model as such the total surface current includes the geostrophic and wind drift flow (as well as other non-geostrophic flows). The geostrophic currents and the total surface currents are used to depict the circulation and to estimate the magnitude of equatorward flow. Geostrophic currents and total surface currents are compared in order to illustrate the presence of the jet as well as to investigate whether the currents are purely geostrophic. Geostrophic currents are also used to compare the model and satellite data.

2.3.1.1 Mean flow patterns of the Benguela Jet

The time-averaged circulation as depicted in both the geostrophic and total surface currents maps (Figure 2.4 a and b) shows the existence of the equatorward jet current off the Cape Peninsula (34^{o}S) and Cape Columbine (33^{o}S). In the annual mean, in both the geostrophic and total surface currents the jet current extends from Cape Peninsula to Cape Columbine. The jet current is narrow and confined to the continental shelf edge and can therefore be referred to as a shelf-edge jet. The core of the jet is stronger off the Cape Peninsula in both geostrophic currents (0.6 $m.s^{-1}$) and total surface currents (0.7 $m.s^{-1}$). However off the Cape Columbine the jet current in both the geostrophic and total surface currents is 0.5 $m.s^{-1}$. To investigate whether the current is predominantly geostrophic or not, the geostrophic currents are subtracted from total surface currents (Figure 2.4 c). Total surface currents are predominantly stronger everywhere with strength of 0.08 $m.s^{-1}$ west off the Cape Columbine. However over the region of Cape Point, total surface currents are about 0.01 $m.s^{-1}$stronger than geostrophic currents.

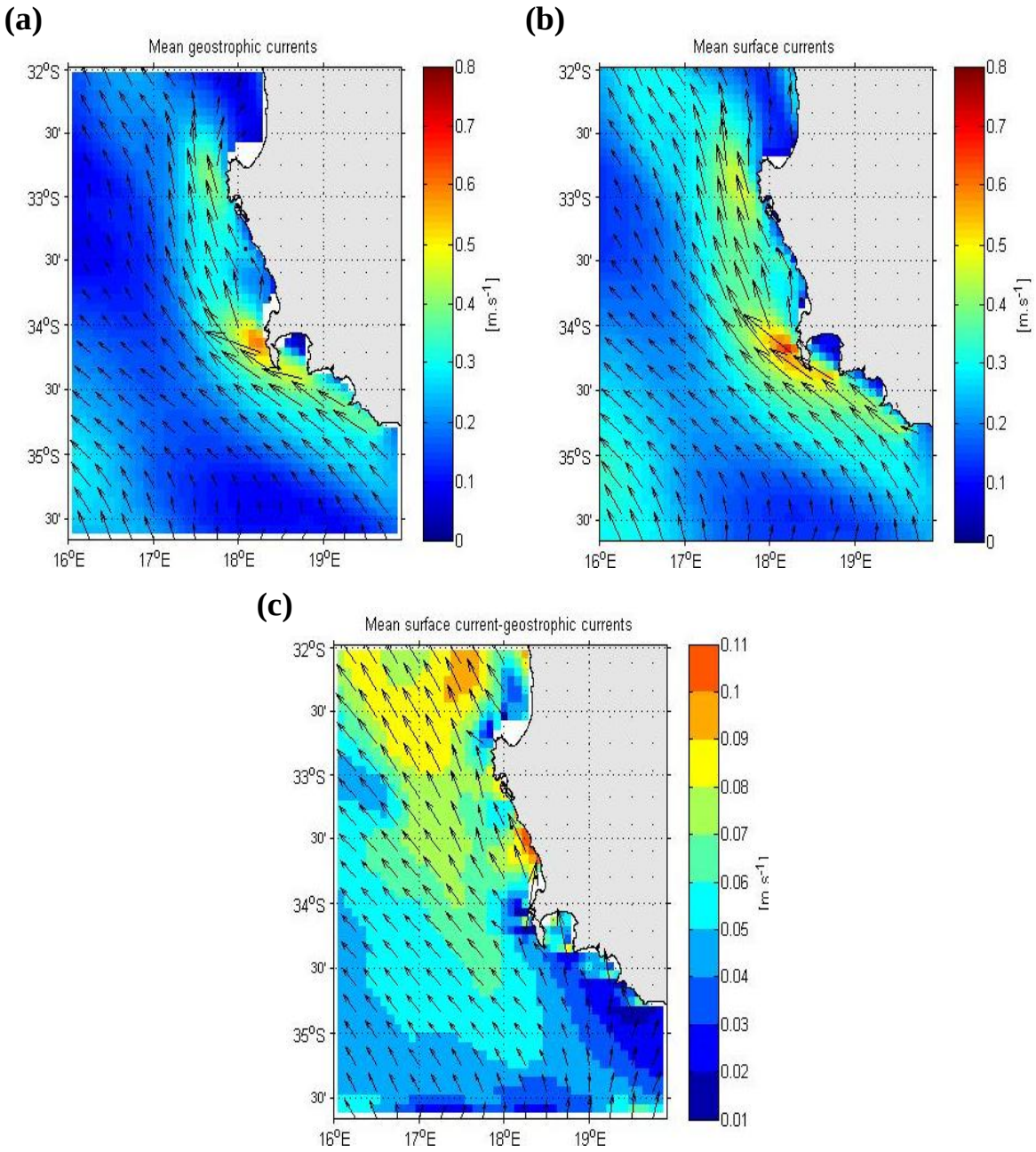

Figure 2.4. *Annual mean of (a) geostrophic currents and (b) total surface currents from the model (ROMS) climatology data c) Difference between estimated total surface currents and geostrophic currents (surface-geostrophic). Arrows indicate the direction of the current flow residual and the background colour shows the intensity of the current residual in the southern Benguela. Units in m.s^{-1}.*

2.3.1.2 Seasonal cycle

The geostrophic and total surface currents illustrate the equatorward jet current off the Cape Peninsula and Cape Columbine in both January and July (Figure 2.5).

In January both the geostrophic and total surface currents show the jet extending from Cape Agulhas to Cape Columbine (Figure 2.5 a and c). The jet is intense and present in January off Cape Peninsula for both geostrophic (0.6 $m.s^{-1}$) and total surface currents (0.75 $m.s^{-1}$). The jet remains close to the coast off the Cape Peninsula (34^{o}S) and veers towards the west and away from the shore at Cape Columbine (33^{o}S) in both total surface and geostrophic currents (Figure 2.5 a and c). In both total surface and geostrophic current maps, there is a split of the current into coastal and offshore branches off Cape Columbine. Total surface currents display a stronger jet at the Cape Peninsula with speeds of 0.75 $m.s^{-1}$ compared to the geostrophic current with speeds of 0.6 $m.s^{-1}$ in January and is generally stronger and wider due to strong south-easterly winds.

In July the jet is confined to the coast and is stronger off the Cape Peninsula (0.5 $m.s^{-1}$) compared to Cape Columbine (0.4 $m.s^{-1}$) in both geostrophic and total surface currents. It is just the coastal part which exists at 33^{o}S (Figure 2.5 b and d). The jet is weaker and narrower off Cape Columbine in both the total surface and geostrophic currents.

Figure 2.6 a and b shows the difference between total surface current and geostrophic current. Positive (negative) values refer to regions where total surface currents are greater (less) than geostrophic current. This shows that total surface currents are stronger than geostrophic currents in January. In July, over the jet area, total surface currents are stronger than the geostrophic currents whereas south of the Cape Peninsula total surface currents are weaker.

Figure 2.7 presents the model derived geostrophic currents and sea surface temperatures for January and July. This depicts the cold upwelled waters and upwelling front. The upwelled cold water is pronounced in January and extends farther offshore. This corresponds to the shift of the jet current farther offshore. While in July the upwelled cold water is weaker and confined to the coast.

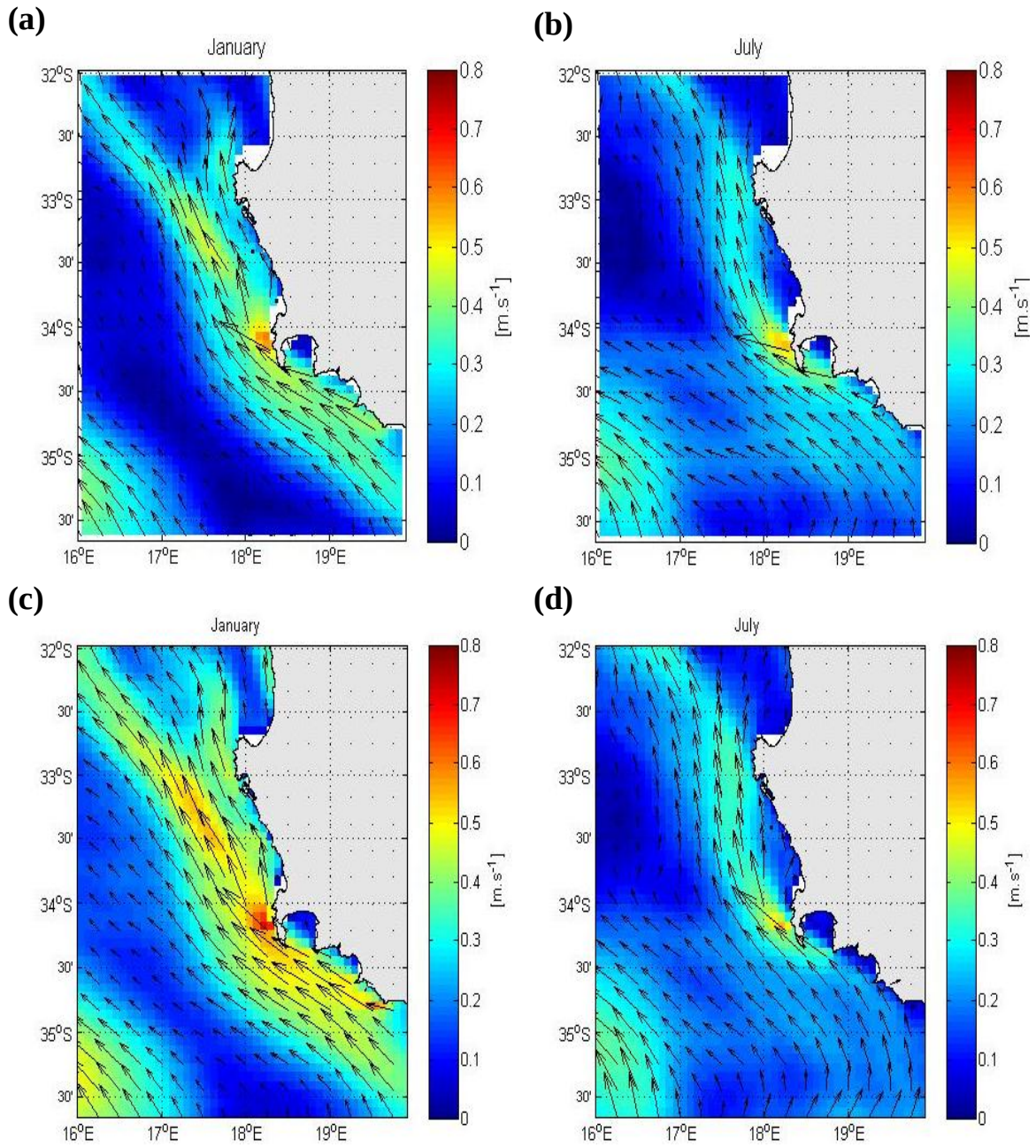

Figure 2.5. *Geostrophic velocities for June and July (a and b) and total surface currents for June and July (c and d) based on model (ROMS) climatology data. Units m.s^{-1}. Arrows indicate the direction of the current flow and the background colour shows the intensity of the current in the southern Benguela.*

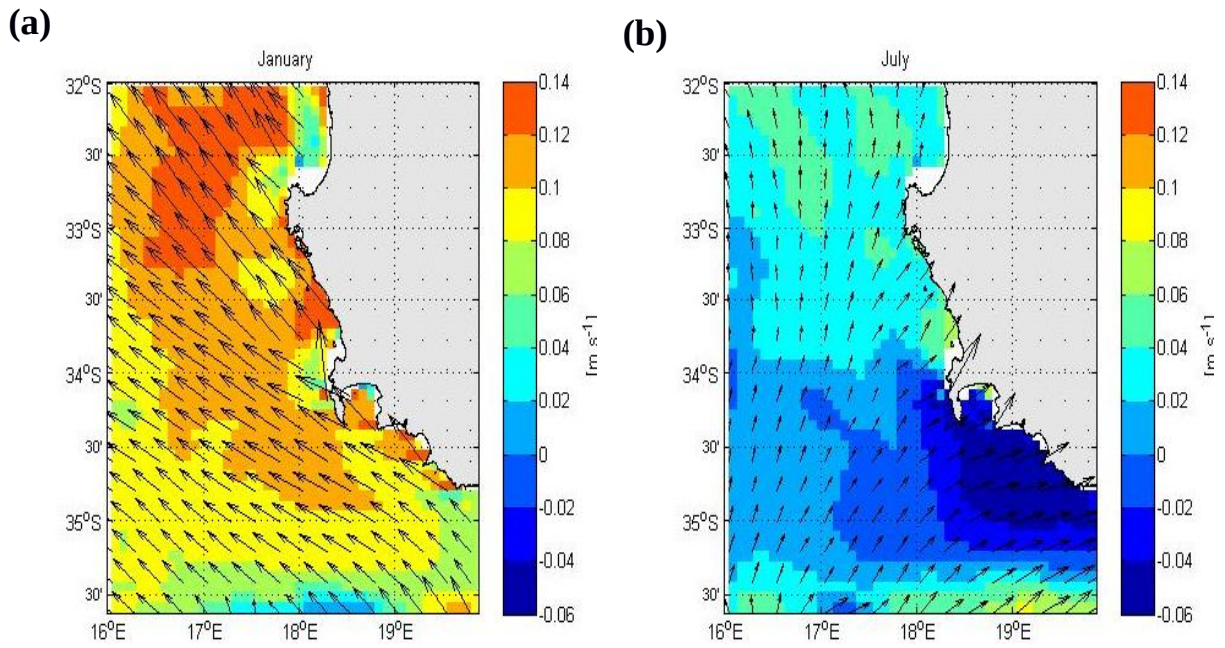

Figure 2.6. a*) and b). Difference between estimated total surface currents and geostrophic currents (total surface-geostrophic) a) January and b) July from the model (ROMS) climatology. Units m.s^{-1}. Arrows indicate the direction of the current flow residual and the background colour shows the intensity of the current residual in the southern Benguela. Units in m.s^{-1}.*

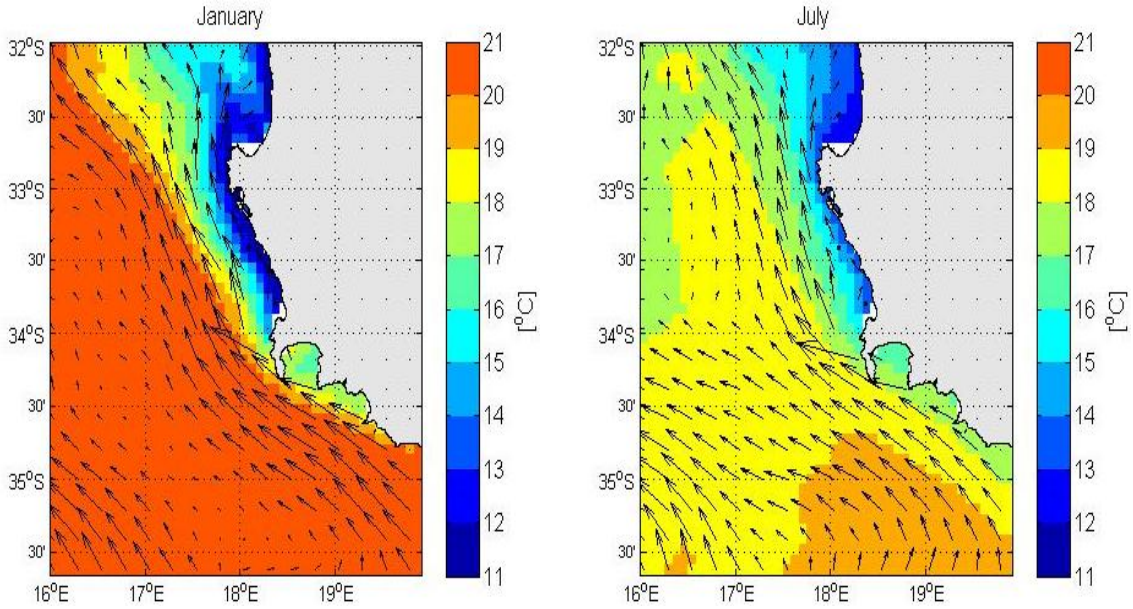

Figure 2.7. *Model (ROMS) climatology geostrophic currents (arrows) and sea surface temperature (°C) for January and July for the southern Benguela region.*

2.3.2 Benguela Jet current based on satellite altimetry

Monthly climatological means were computed for each altimetry mission. For the altimeter tracks 8 years of data from J1_209 and 11 years from Tp_209 were available whereas only 4 years of data were available for J1_31 and Tp_31. The geostrophic velocities were computed from these monthly climatological means in an attempt to highlight the presence of the Benguela Jet current (Section 2). Monthly climatologies of SST were computed from 11 years of SST information retrieved from MODIS.

2.3.2.1 Mean flow patterns of the Benguela Jet

Figure 2.8 illustrates the annual mean geostrophic currents derived from the altimeter tracks. The geostrophic currents derived from the Jason1A show dominant north-westward flowing currents with a stronger narrow current (0.6 $m.s^{-1}$) between the 200 m and 500 m isobaths and a weaker (0.2 $m.s^{-1}$) south-eastward current shoreward. This suggests the presence of a strong jet current between these isobaths as a strong narrow annual feature of the southern Benguela upwelling region. Figure 2.8 b, based on Topex-A depicts a stronger north-westward current offshore of the 500 m isobaths as compared to the geostrophic current derived from Jason1A.

Jason1B and Topex-B altimeter tracks derived mean geostrophic current also illustrates the north-westward current with weaker currents dominating south off Cape Point based on Topex-B derived geostrophic currents. Both tracks depict a strong north-westward current near the 500 m isobaths. These tracks capture the offshore boundary of the jet, depicting the annual existence of the jet further offshore. However due to land contamination the J1_31 and Tp_31 tracks fail to resolve the jet when the jet is closest to the coast.

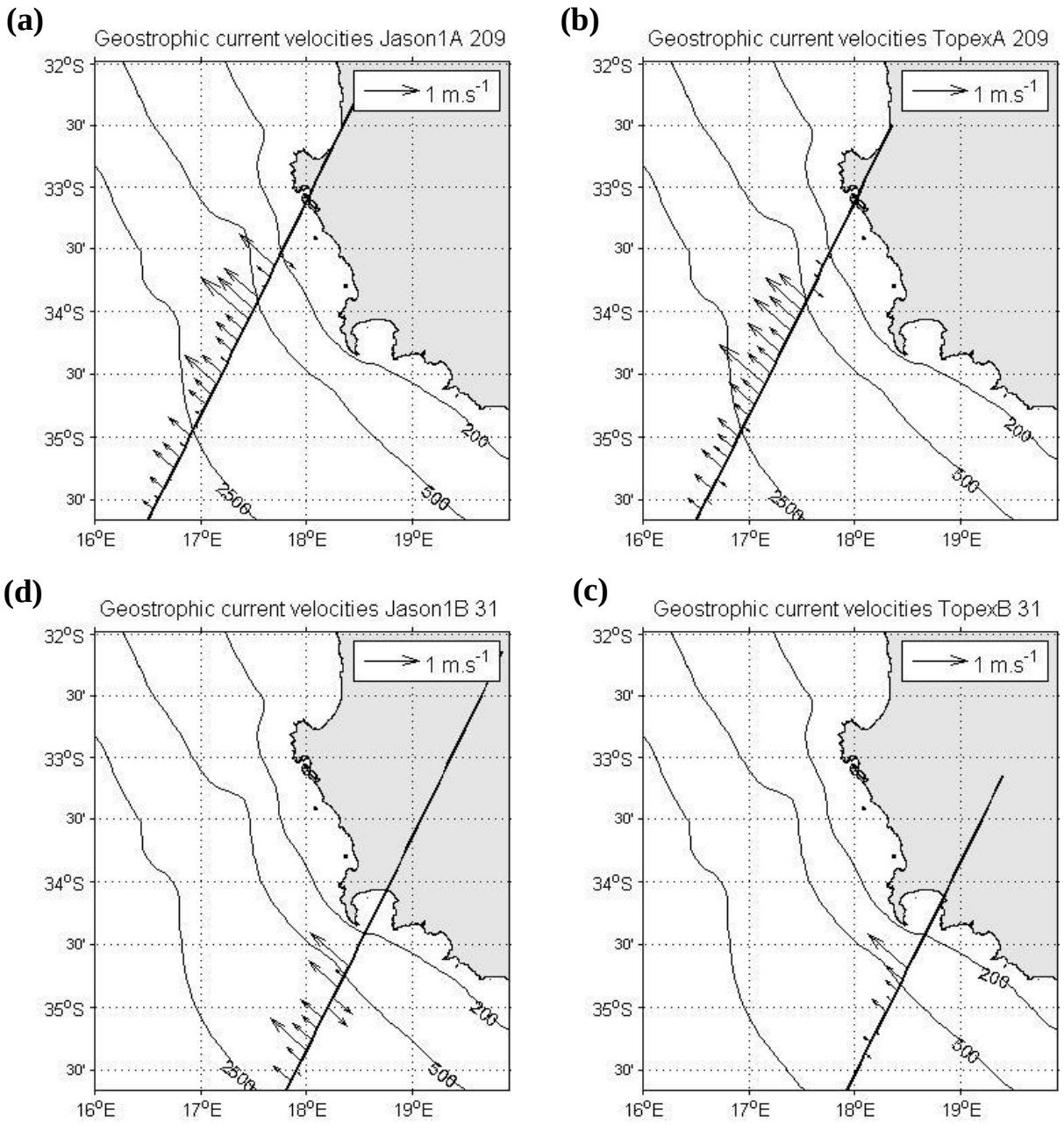

Figure 2.8. *Annual mean geostrophic currents (arrows) derived from Jason1 (a and c) and Topex (b and d) satellite altimetry. Units in m.s^{-1}. The 200, 500 and 2500 isobaths are shown. The solid line indicates the tracks of Jason and Topex missions crossing Cape Columbine and south of Cape Point in the southern Benguela region. The annual mean was derived from 8 years of Jason1A 209, 11 years of TopexA 209 and 4 years of both JasonB 31 and TopexB31 altimeter data.*

2.3.2.2 Seasonal cycle

SST and Altimetry SSH gradients for January and July are used to highlight regions of stronger surface current flows (Figure 2.9 a-d). The gradients were calculated starting from west to east resulting in the negative (southward flow) and positive (northward flow) gradients (as shown in figure 2.9-2.10). Regions of strong SST and SSH gradients are expected to indicate the position of the front and the Benguela Jet with a stronger gradient associated with increased flow. Longitudinal shifts in the region of maximum gradient will also help to clarify if the jet moves with seasons.

J1_209 exhibits a northward flow between 17.4-17.6^{o}E in both January and July although the SST gradient is positioned slightly further to the east than the SSH gradient (Figure 2.9 a-b). The SST gradient is also less well-defined in July, having a more gradual slope. This depicts the presence of the jet as a northward current between 17.4-17.6^{o}E, off Cape Columbine. The jet is also evident in the Tp_209 SSH and SST gradient (Figure 2.9 c and d). SST gradient is strongest in January between 17.5 and 17.6^{o}E and in July the gradient is weaker and less defined. The SSH gradient is broader in July (Figure 2.9 b and d), implying a less defined, broader jet.

Figure 2.10 shows the SST and SSH gradients derived from J1_31 and Tp_31 against longitude. The SST and SSH gradients for both J1_31 and Tp_31 show a northward flow between 18-18.2^{o}E in January, showing the presence of the jet at these position. In July these tracks fail to resolve the jet due to the fact that the altimetry dataset suffers from contamination closer to the shore.

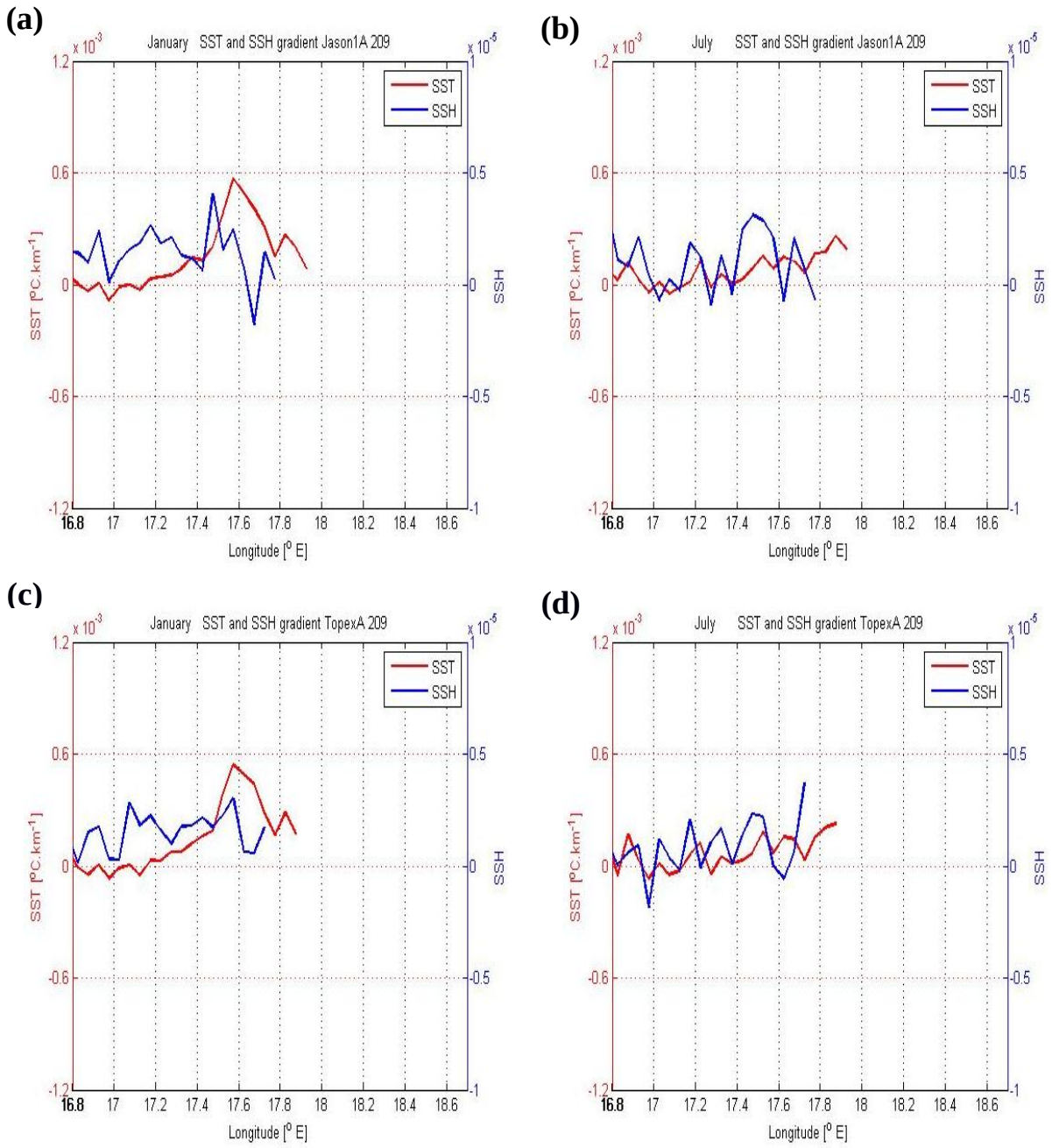

Figure 2.9. *Climatological sea surface temperature ($^{o}C.km^{-1}$) and sea surface height gradients against longitude (^{o}E) for January (Left) and July (Right) from Jason-1A (a-b) and Topex-A (c-d) track 209. Negative gradients indicate southward flow and positive gradients northward flow. Regions of strong SST and SSH gradients are expected to indicate the frontal position of the Benguela Jet.*

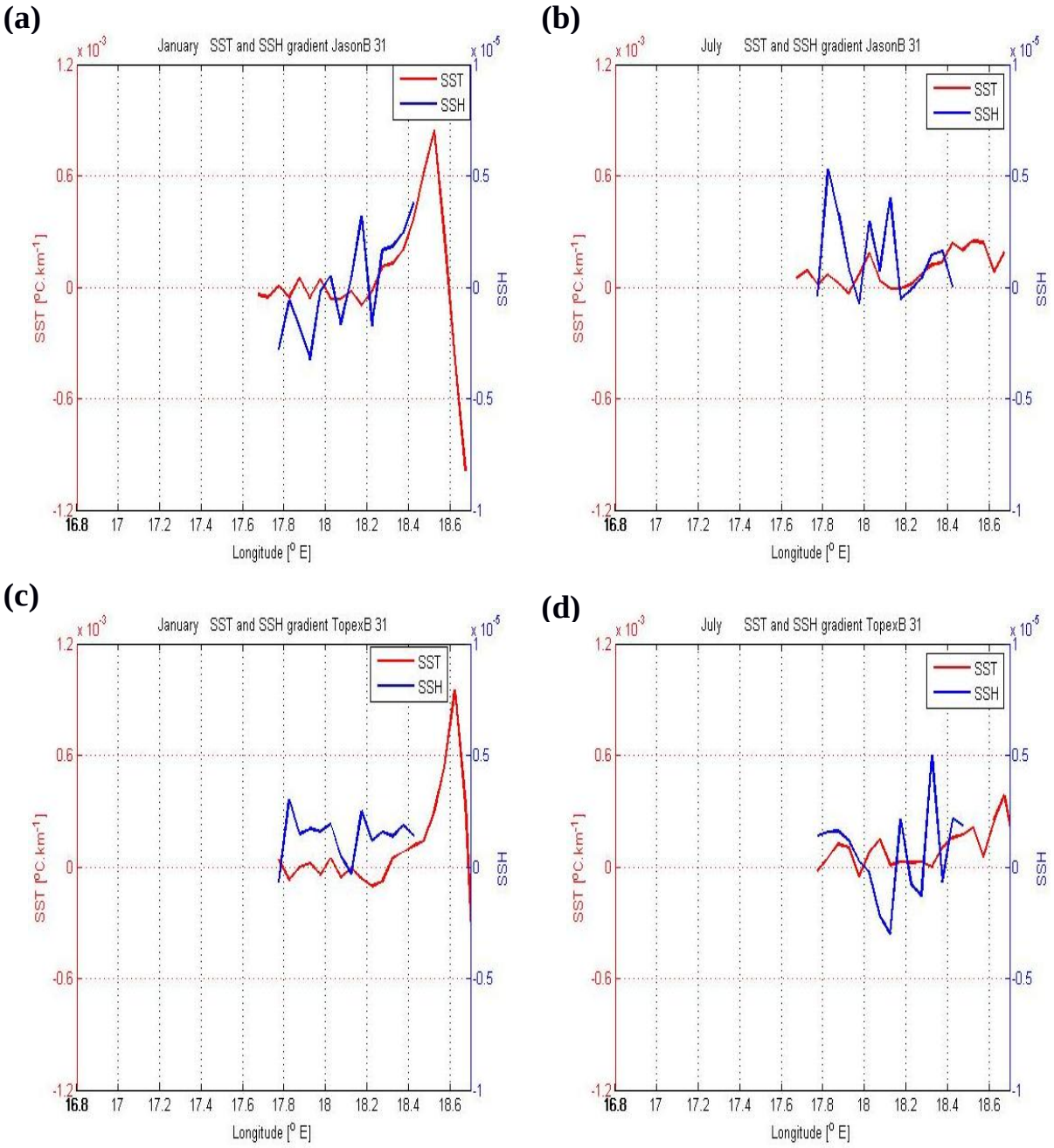

Figure 2.10. *Climatological sea surface temperature ($^oC.km^{-1}$) and sea surface height gradients against longitude (^oE) for January (Left) and July (Right) from Jason-1B (a-b) and Topex-B (c-d) track 31. Negative gradients indicate southward flow and positive gradients northward flow. Regions of strong SST and SSH gradients are expected to indicate the frontal position of the Benguela Jet.*

Figure 2.11 shows geostrophic velocities and the direction of the flow in January and July. Geostrophic currents calculated from Jason-1A are predominately north-westward flowing with a weaker south-eastward current closer inshore (Figure 2.11 a-b). The current is stronger and further offshore in January as compared to July. This depicts the Benguela Jet as a seasonally varying flow, with a stronger and narrower jet positioned further west during the austral summer. The inshore south-eastward current is stronger in January when the jet is further offshore.

The geostrophic current estimated from Topex-A shows a defined north-westward flow (Figure 2.11 c). In January the position of the jet is around the 500 m isobath and between 200 m and 500 m isobaths in July. In both Jason-1A and Topex-A the stronger currents are located between the 200 m and 500 m isobaths depicting the position of the jet. The altimeter data for all the missions illustrate a maximum surface velocity of 1 $m.s^{-1}$ in the climatological mean (Figure 2.11 and 2.12). In January the speed of the jet is 0.6 $m.s^{-1}$ in both the J1_209 and Tp_209 tracks. In July, J1_209 and Tp_209 show a weaker jet with 0.4 $m.s^{-1}$. The geostrophic velocities computed from the Jason-1B and Topex-B altimeter missions also show a dominant equatorward flow and a region of south-eastward flow (Figure 2.12). In January the geostrophic currents derived from Jason-1B capture the offshore part of the jet. However in July neither tracks show the presence of the jet current. This could be due to the fact that the jet is closest to the shore and therefore the altimetry data is flagged as bad data near the coast.

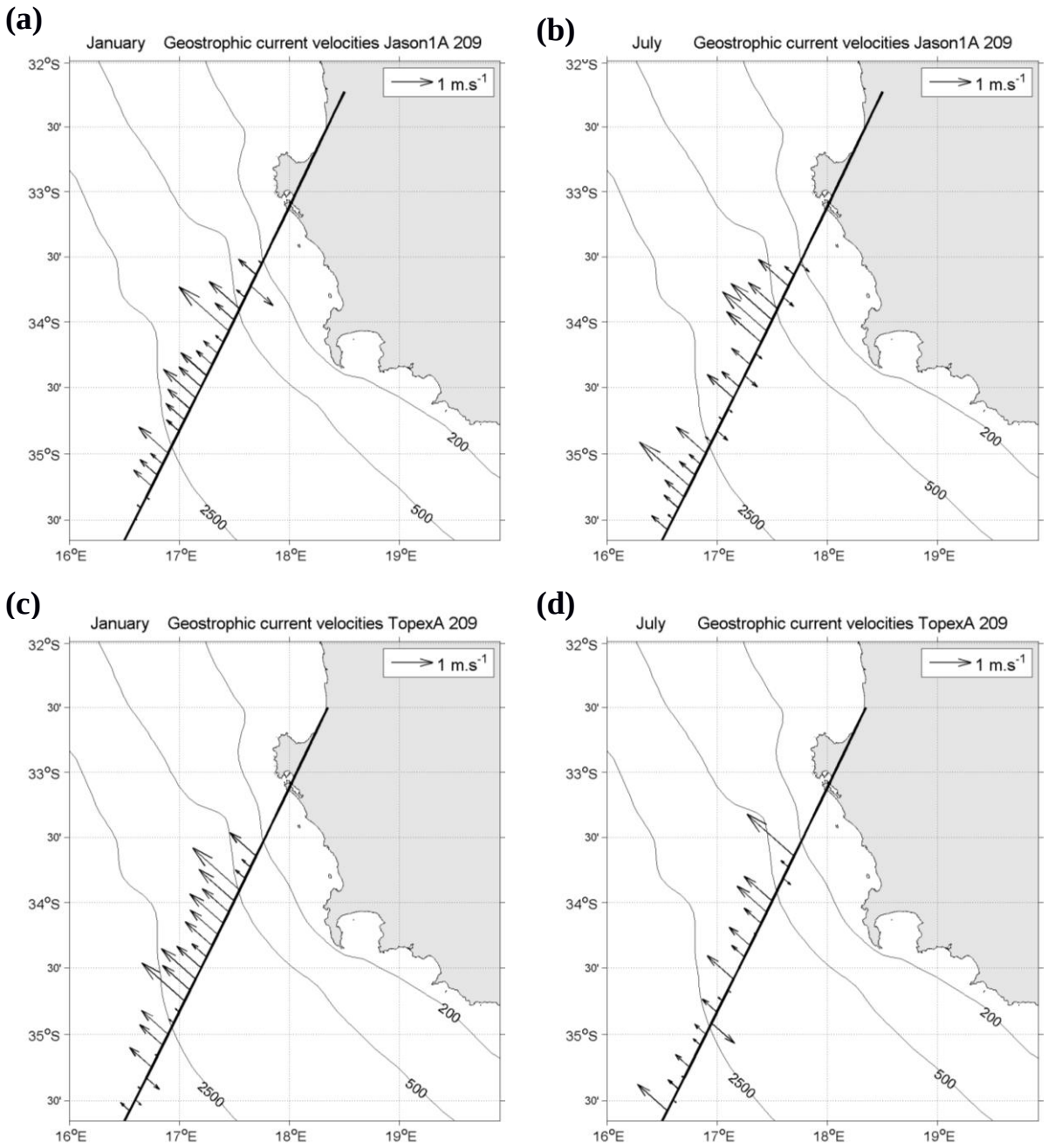

Figure 2.11. *Geostrophic velocities (arrows) (m.s^{-1}) for January (left) and July (right) computed from Jason-1A track 209 (a-b) and Topex-A track 209 (c-d) satellite altimeter data climatology. The 200, 500 and 2500 isobaths are shown. The solid line indicates the tracks of Jason and Topex missions crossing off Cape Columbine in the southern Benguela region.*

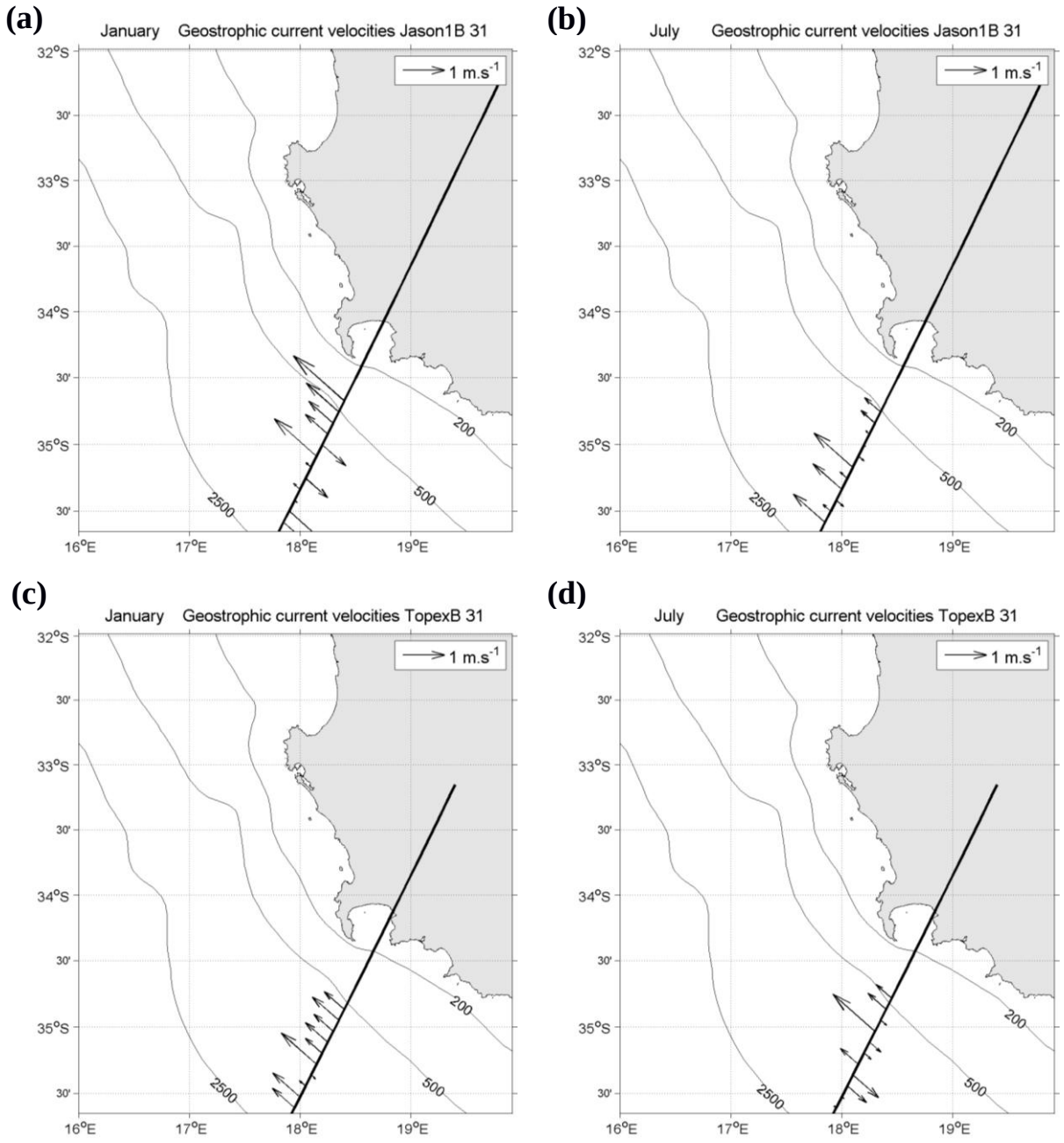

Figure 2.12. *Geostrophic velocities (arrows) (m.s^{-1}) for January (left) and July (right) computed from Jason-1B (a-b) track 31 and Topex-B (c-d) track 31 satellite altimeter data climatology. The 200, 500 and 2500 isobaths are shown. The solid line indicates the tracks of Jason and Topex missions crossing south of Cape Point in the southern Benguela region.*

The climatological geostrophic velocities based on J1_209 and Tp_209 altimeter tracks were averaged over the region 17.4°E-17.6°E (Figure 2.13). Six vectors were averaged over this region. The region was selected based on the gradient analysis (Figure 2.9), in order to further investigate if there was a seasonal signal within the region where the jet usually resides.

The Jason-1A averaged geostrophic velocities show maximum velocities of 0.32 $m.s^{-1}$ in December and in July with a velocity of 0.31 $m.s^{-1}$. However the month of August shows a minimum velocity of 0.16 $m.s^{-1}$. Topex-A shows peak velocities in January (0.28 $m.s^{-1}$) and in December (0.32 $m.s^{-1}$). Monthly variations in the climatological current speeds extracted from these altimetry tracks are small. These tracks do not depict a seasonal signal of the Benguela Jet current (Figure 2.13).

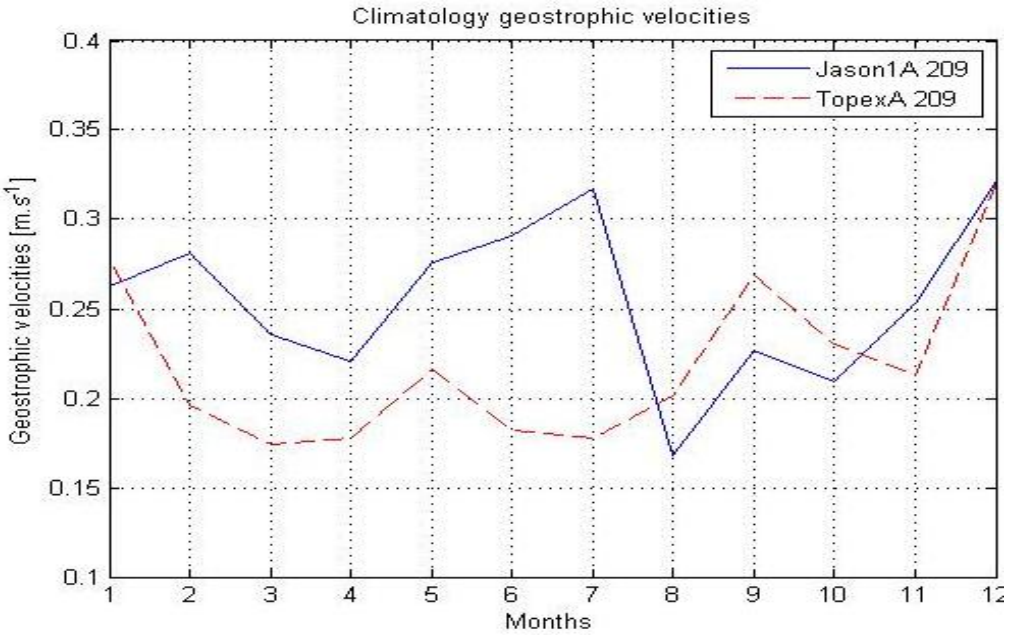

Figure 2.13. *Climatology of geostrophic velocities averaged within longitudes 17.4°E-17.6°E and derived from the Jason1 (blue) and Topex-A (red) datasets. Units $m.s^{-1}$.*

2.3.3 Comparison of satellite observations and model output.

A map of the geostrophic current over the study region was derived from the numerical model's sea surface height climatology (as described in Section 2). The across geostrophic currents were computed from the ADT climatology for each altimetry mission. In this subsection the geostrophic currents based on the satellite altimeter are compared to the model-derived geostrophic currents. The model-derived geostrophic currents were extracted along the altimeter tracks in order to better compare with satellite-derived geostrophic

currents. It is important to note that only the current flowing perpendicular to the satellite altimeter track is reproduced when deriving the geostrophic velocities. The model has a high resolution of 9 km.

The geostrophic currents estimated from the satellite altimeter and model output data display a strong dominant north-westward current flow (Figure 2.14-2.15). The altimeter-derived geostrophic current for all the tracks also show a south-eastward current, which is not present in the model. The model, J1_209 and Tp_209 tracks are consistent in depicting a narrow-fast jet current in January and weaker broader jet current in July; however the positioning of the current is slightly different. The geostrophic current based on the model illustrates a strong surface current between the 200 m and 500 m isobaths off False Bay (Figure 2.15) which is not resolved by both the J1_31 and Tp_31 in July due to data contamination close to the coast.

To further compare the monthly climatology, geostrophic current velocities derived from both model and satellite observations, are plotted in hovmöller plots (Figure 2.16-2.17). Jason-1A shows a strong northward current between 17.4^{o}E - 17.6^{o}E. This is consistent with the SST and SSH gradient presented in subection 2.3.2 (in Figure 2.13). The current is stronger in January to March with maximum velocity of 0.5 m.s^{-1} and a minimum velocity in August (0.3 m.s^{-1}). Topex-A also shows a northward current at the same position with a maximum velocity of 0.4 m.s^{-1} in November, December, January and February also in September. Model data extracted along the J1_209 and Tp_209 tracks shows a stronger northward current between 17.4-17.8^{o}E with maximum velocity of 0.5 m.s^{-1} in September. Geostrophic currents derived from the altimetry resolves the presence of the Benguela Jet in the J1_209 and Tp_209 tracks which depicts a stronger northward flow between 17.4 -17.6^{o}E.

Compared to J1_31 and Tp_31 in Figure 2.16 (c and d) the model illustrates a stronger northward flow between 18.4-18.6^{o}E (Figure 2.17 c and d). The current is stronger from January to April (0.5m.s^{-1}), minimum in May to July (0.4 m.s^{-1}) and then strengthen again in August to December. The current velocities estimated with the altimetry are within same range as those from the model. This suggests that the model is able to resolve the Benguela Jet, although the geostrophic velocities derived from the model strongly shows northward currents.

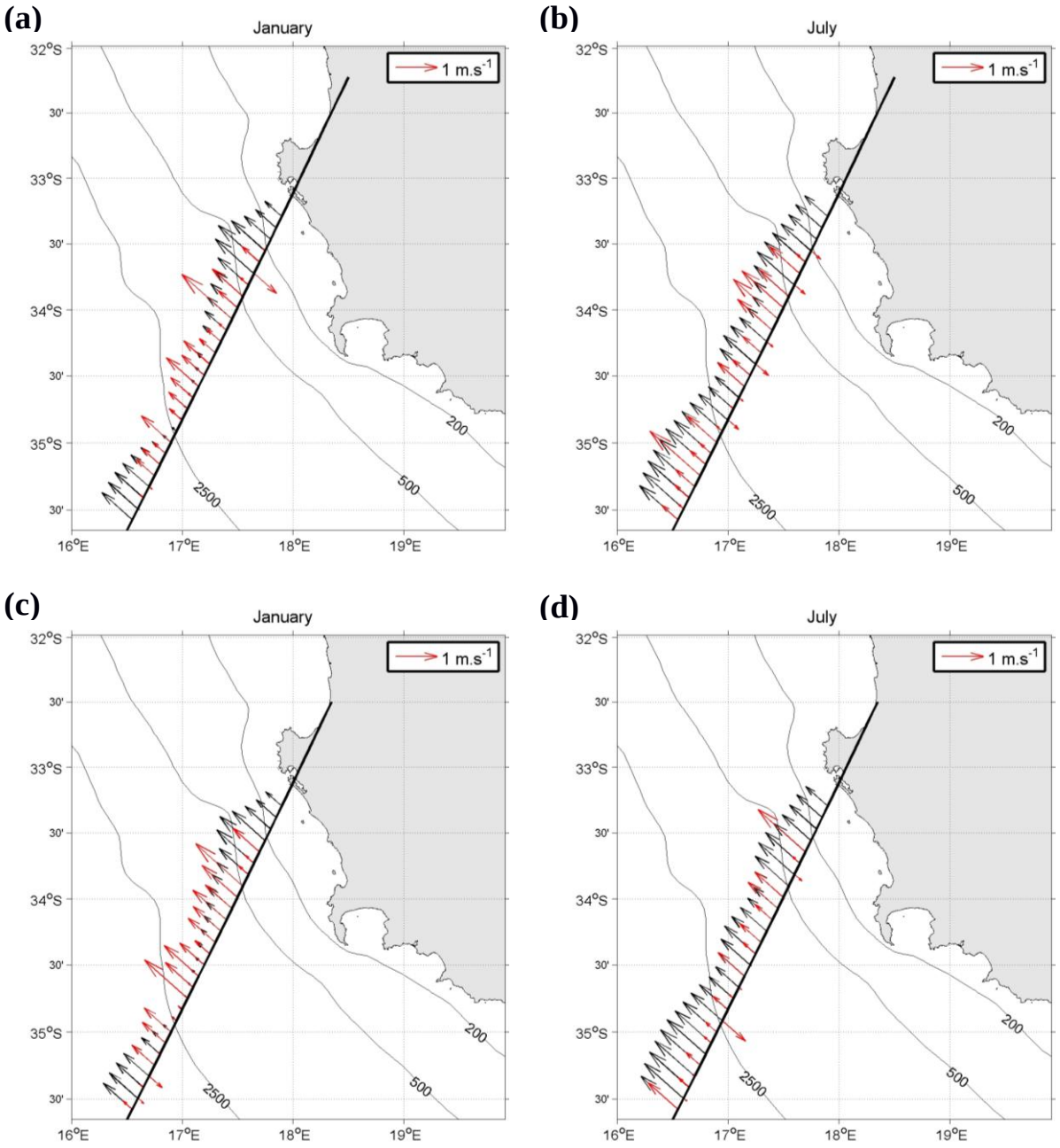

Figure 2.14. *Geostrophic velocities (arrows) (m.s^{-1}) for January (left) and July (right) computed from model (black arrows) and Jason-1A (a-b) and Topex-A (c-d) track 209 (red arrows) satellite altimeter data climatology. The 200, 500 and 2500 isobaths are shown. The solid line indicates the tracks of Jason and Topex missions crossing Cape Columbine in the southern Benguela region. Model data were extracted along the tracks for better comparison with satellite altimetry data.*

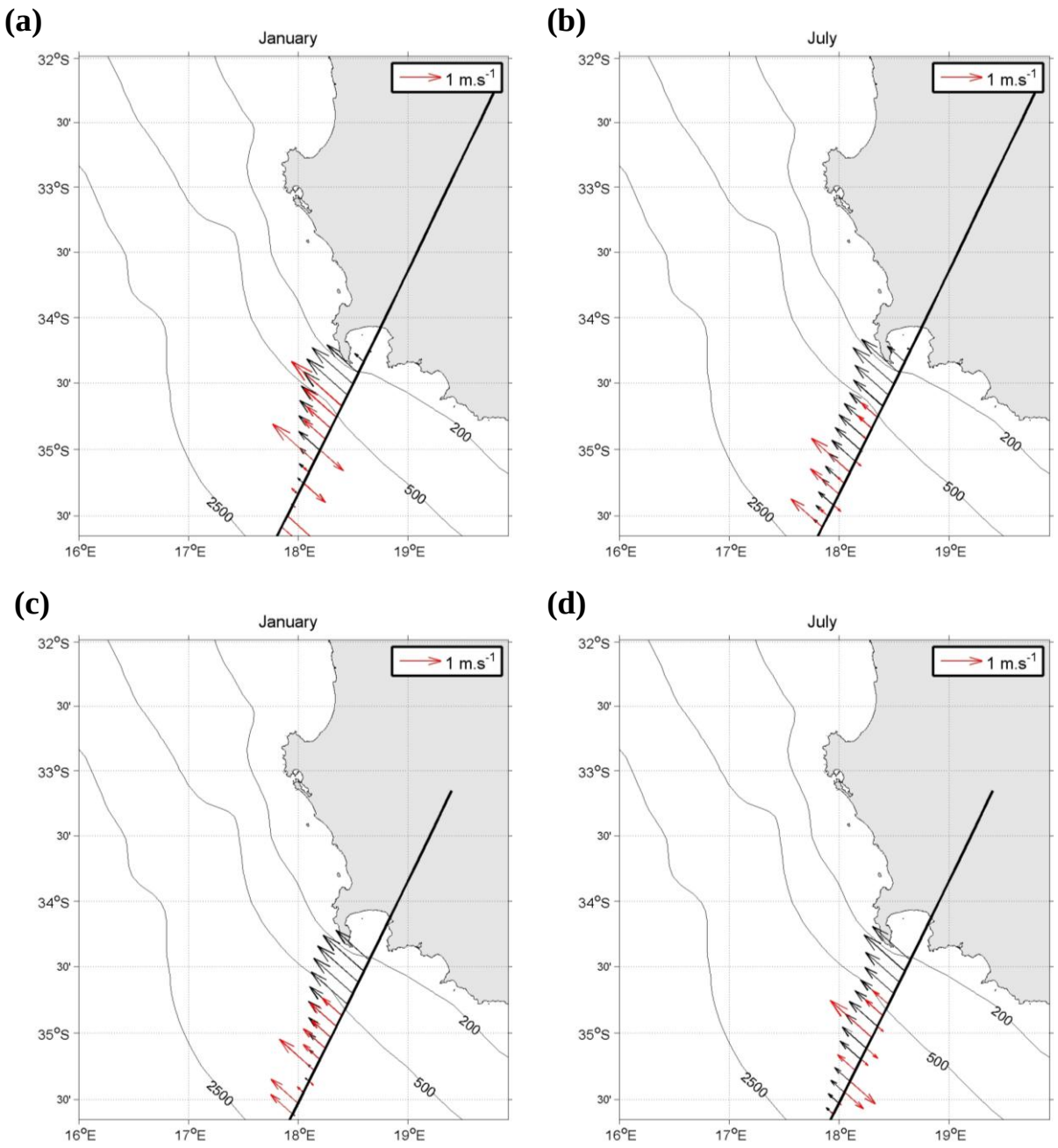

Figure 2.15. *Geostrophic velocities (m.s^{-1}) for January (left) and July (right) computed from model (black arrows) and Jason-1B (a-b) and Topex-B (c-d) track 31 (red arrows) satellite altimeter data climatology. The 200, 500 and 2500 isobaths are shown. The solid line indicates the tracks of Jason and Topex missions crossing south of Cape Point in the southern Benguela region. Model data were extracted along the tracks for better comparison with satellite altimetry data.*

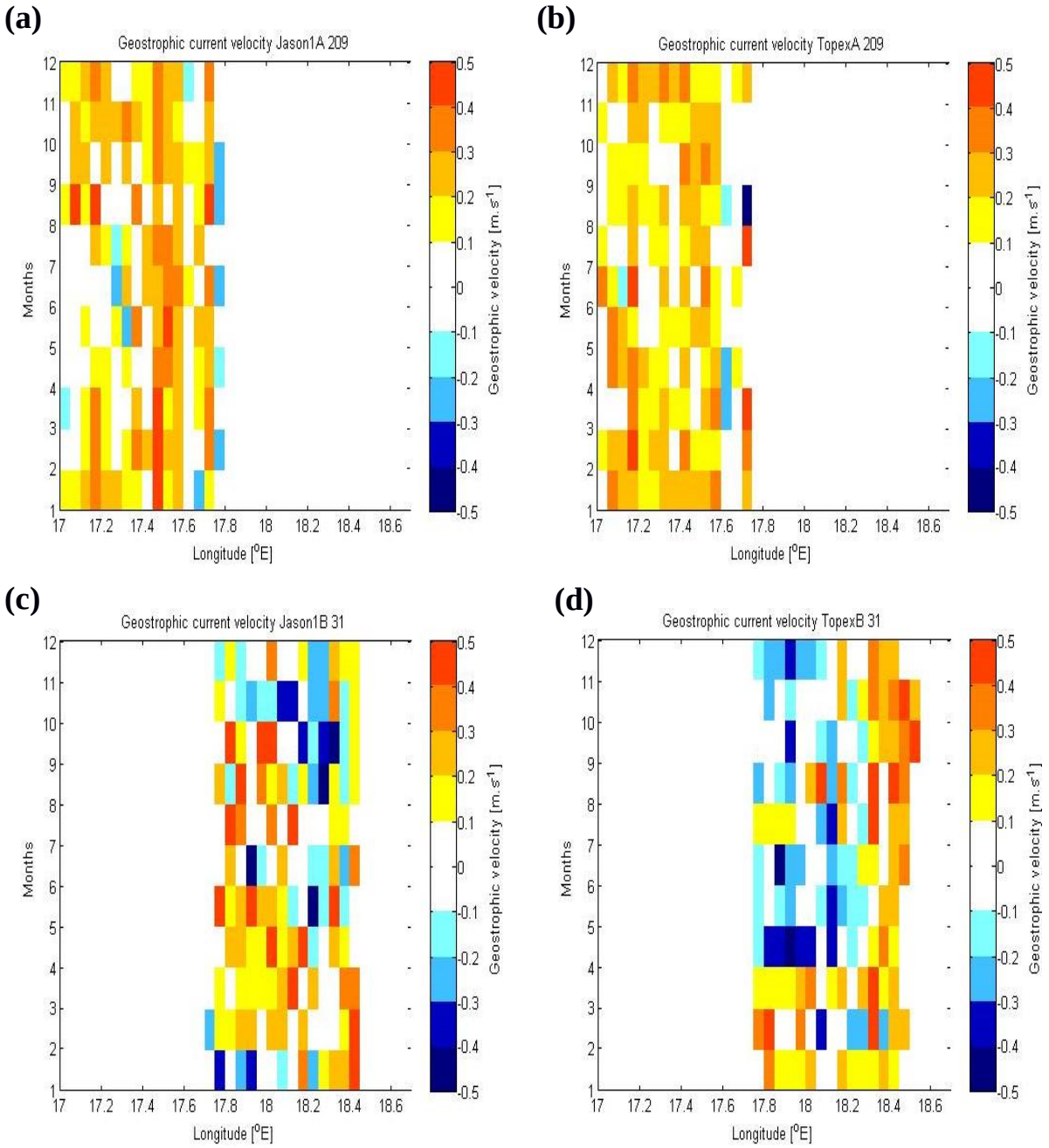

Figure 2.16. *Time-longitude plot of the cross-track geostrophic current climatology based on (a) Jason-1A,(b) Topex-A track 209 and based on (c) Jason-1B and (d) Topex-B track 31. Positive values indicate northward currents and negative indicate southward currents. Units in* $m.s^{-1}$.

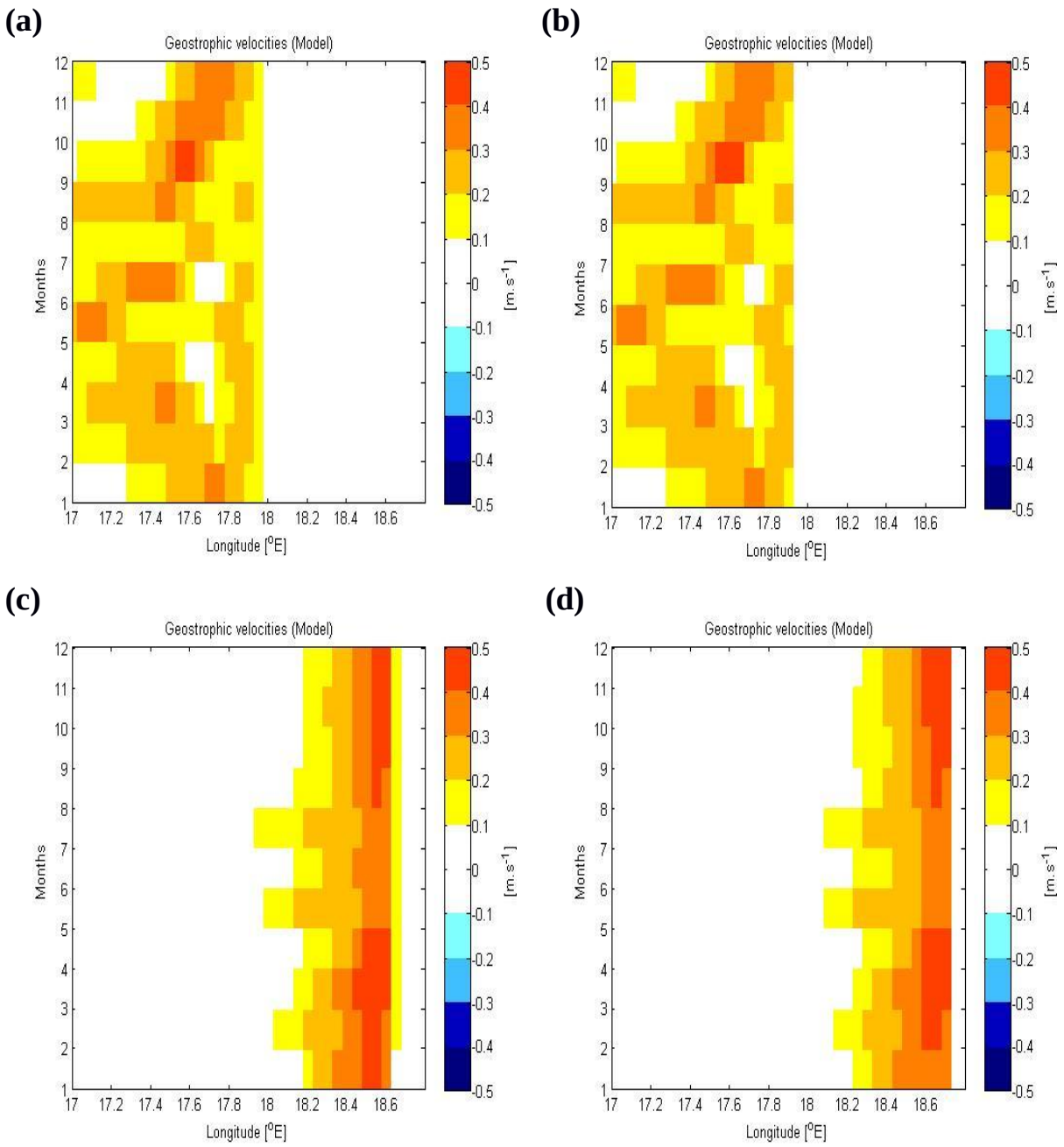

Figure 2.17. *Time-longitude plot of the model geostrophic current climatology extracted along the tracks of (a) Jason-1A, (b) Topex-A,(c) Jason-1B and (d) Topex-B. Units in m.s^{-1}. Positive values indicate northward currents and negative indicate southward currents.*

The vertical section plots of January and July shown in Figure 2.18 and 2.19 were extracted from the model (ROMS) along each altimeter track. The strongest current velocities of about 0.4 $m.s^{-1}$ in January are at the surface for both Jason1A 209 and TopexA 209. In Janaury, the weakest current of 0.1 $m.s^{-1}$ is within the 100 m depth closer to the coast whereas further offshore the current is below 500 m depth based on Jason1A 209. While based on TopexA 209 the weakest current (0.1 $m.s^{-1}$) is approximately at 200 m depth closer to shore and below 500 m depth further offshore . In July both the Jason1A 209 and TopexA 209 show the weakest current (0.1 $m.s^{-1}$) to be closer to the surface near the coast and extends below the 500 m depth further offshore (Figure 2.18 b and d). The poleward undercurrent is absent in all the vertical section plots.

In January both Jason1B and TopexB display are stronger current velocity (0.4 $m.s^{-1}$) at the surface, with a weaker current (0.1 $m.s^{-1}$) extending to 300 m depth (Figure 2.19 a and c). While in July currents with velocities of about 0.3 $m.s^{-1}$ is within the top 100 m water depth, with the weakest current (0.1 $m.s^{-1}$) extending to 100 m depth in both altimeters (2.19 b and b). These plots also show that the geostrophic flow is baroclinic respectively.

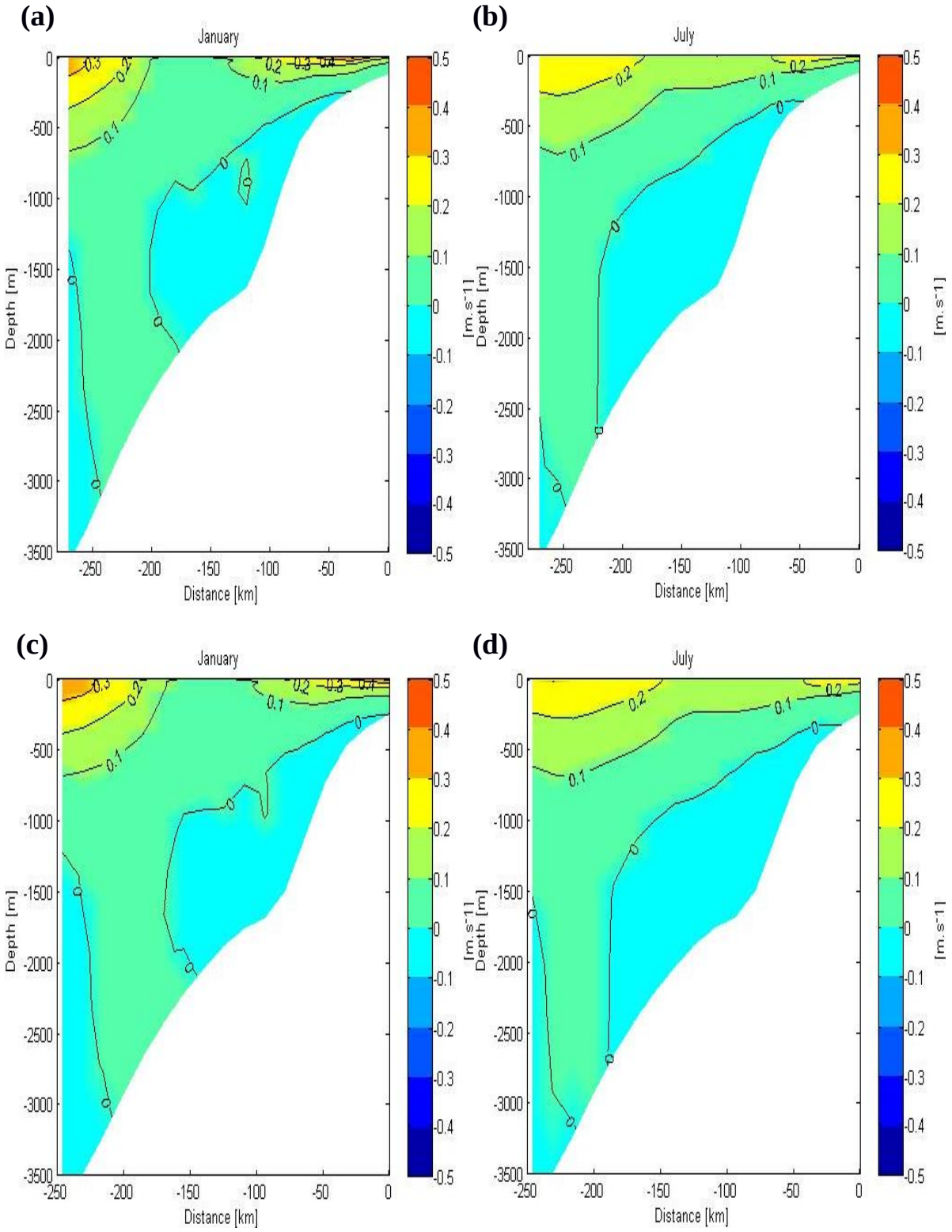

Figure 2.18. *Vertical section of velocities (m.s^{-1}) extracted from the model along the altimeter tracks (a-b) Jason1A 209 and (c-d) Topex A 209 altimeters. Plotted with depth [m] and distance [km] from shore. The colours indicates the intensity of the velocity.*

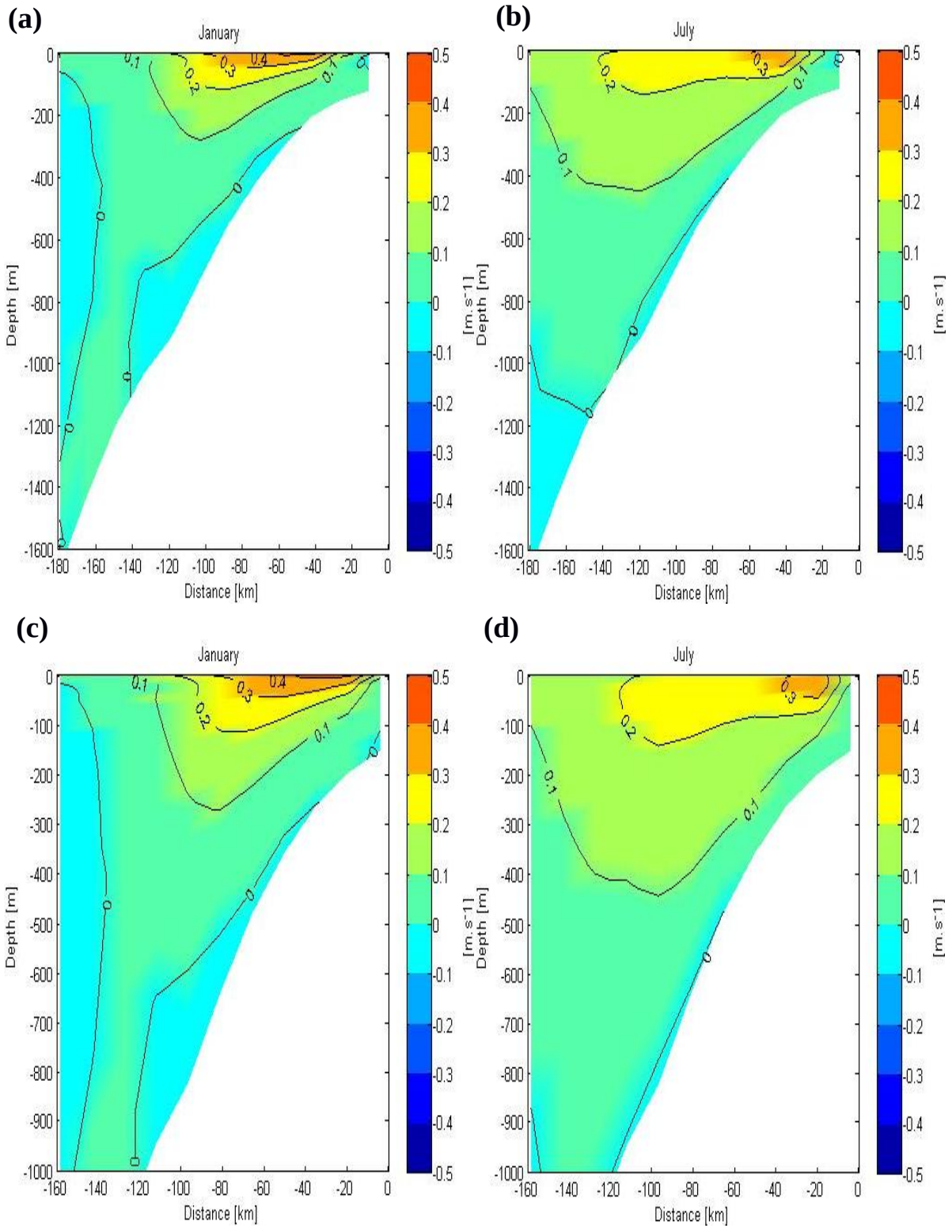

Figure 3.19. *Vertical section of velocities (m.s^{-1}) extracted from the model along the altimeter tracks (a-b) Jason1B 31 and (c-d) TopexB 31 altimeters. Plotted with depth [m] and distance [km] from shore. The colours indicates the intensity of the velocity.*

2.3.4 Interannual variability

Geostrophic currents were also derived using the 10-days instantaneous observation from the different altimeter missions. Hovmöller plots in Figure 2.20 based on surface geostrophic currents are used to illustrate the interannual variability of the jet current and to note if there are variations in any seasonal signals within each year that may weaken the seasonal signal in the climatology.

In 2005 and 2006 between 17.4-17.6^{o}E, a seasonal signal is apparent, with strong flow in January (0.6 m.s^{-1}) and a flow of 0.4 m.s^{-1} in June-August based on the Jason-1A derived geostrophic velocities (Figure 2.20 a). Topex-A in 1993 shows a semi-seasonal signal with strong north-westward current in January and June (1 m.s^{-1}) and then an increase in December (0.4m.s^{-1}).

Jason-1B shows a seasonal signal in 2010 at 18^{o}E with stronger currents in January (0.6m.s^{-1}) and weaker current in July (0.2 m.s^{-1}). The altimeter data shows a seasonal cycle but not always a strong one.

Figure 2.20 (a), also shows stronger offshore, north-westward current (1 m.s^{-1}) in late 2004 and in 2005 based on the Jason-1A derived geostrophic currents. Whereas, the current derived from Topex-A depicts stronger north-westward current (1 m.s^{-1}) in each year displaying the presence of the Benguela Jet as a year around feature of the southern Benguela in particular off Cape Columbine (Figure 2.20 b). In 1993 the current appears to be closest to inshore.

The altimetry reveals the presence of south-eastward currents to the west of the Benguela Jet. Jason-1B derived geostrophic currents reproduce north-westward currents in 2011 and weaker currents (0.2 m.s^{-1}) in 2010 (Figure 2.20 c). However Topex-B shows a stronger jet (1 m.s^{-1}) in 2003 and 2004.

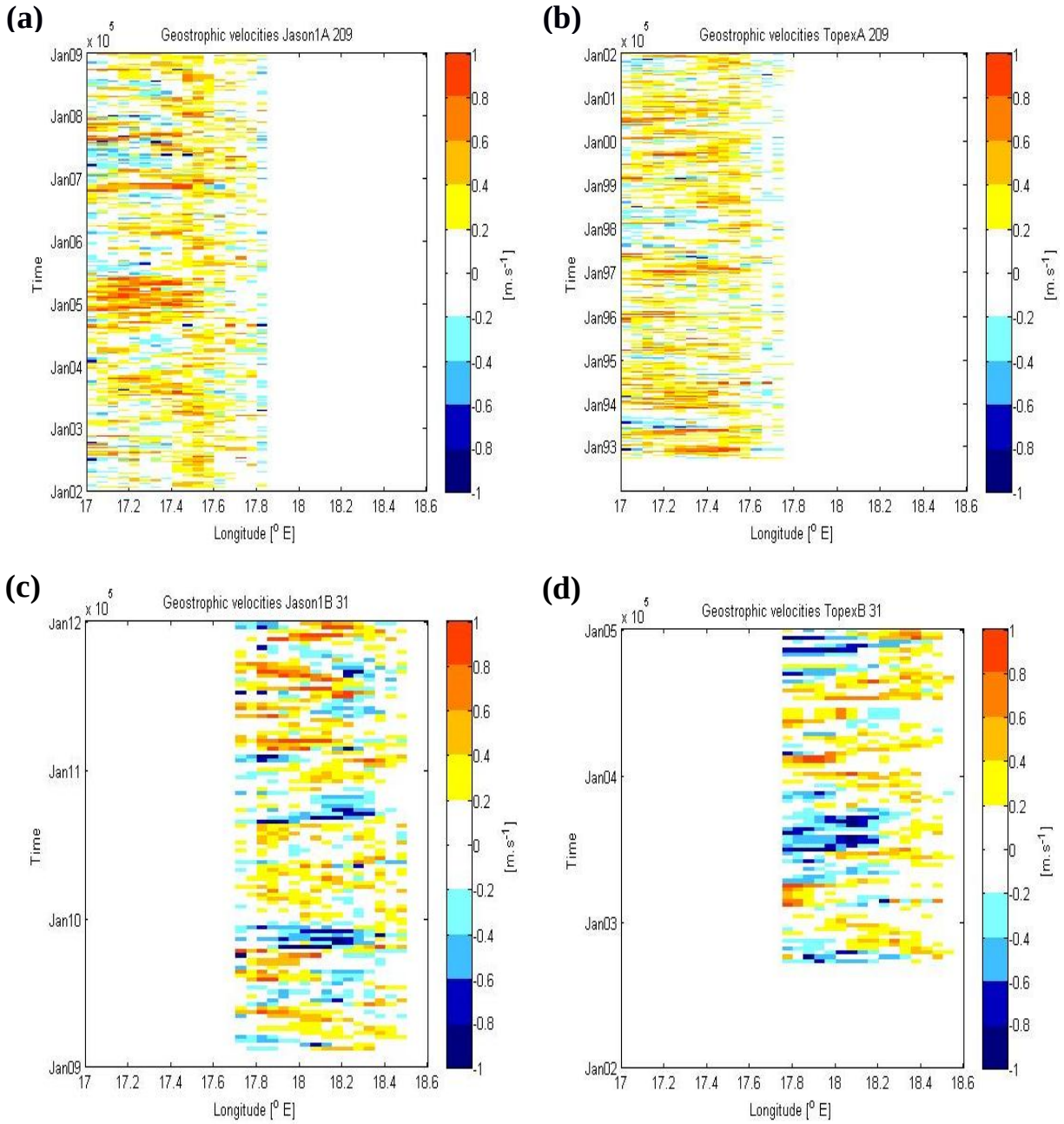

Figure 2.20. *Time-longitude plot of 10 days across-track geostrophic currents derived from (a) Jason-1A, (b) Topex-A, (c) Jason-1B and (d) Topex-B. Units in m.s^{-1}. Positive (negative) values indicate a northward (southward) flow.*

2.4. Discussion

The research presented in this thesis aims to improve our understanding of the Benguela Jet and its annual variability. The study relied on the use of 1) SSH observations from satellite altimeters across both the northern and southern regions of the Benguela Jet, 2) Monthly climatologies of MODIS SST and 3) Current velocity and SSH monthly climatologies derived from the ROMS numerical model (as defined in Section two). The model and the satellite results demonstrated the existence and the temporal variability of the Benguela Jet current.

2.4.1 Mean flow patterns of the Benguela Jet

Previous studies have described the Benguela Jet as an equatorward flowing current that extends from the Cape Peninsula to Cape Columbine in the southern Benguela region with mean velocities of about 0.5 $m.s^{-1}$ (Shannon & Nelson, 1996; Fowler & Boyd, 1998). Mean flow derived from the ROMS model used here, showed the existence of the equatorward jet current extending from the Cape Peninsula to Cape Columbine, with mean velocities of 0.5 $m.s^{-1}$ in agreement with the results of Veitch (2009). The wind set-up the temperature and SSH that drive the current. The difference between the total surface currents and geostrophic currents in the model showed that the jet is predominantly wind driven and less is geostrophic. The jet is geotrophic but much stronger surface current show the importance of Ekman wind drift as part of one driving mechanism for the jet motion in surface layer. The wind is the driving force but different mechanisms occur: Ekman and Geostrophic.

In the altimetry data, J1_209 and Tp_209 tracks resolved the jet between the 200 m and 500 m isobaths off Cape Columbine. The jet was strongly pronounced in the Jason-1A altimeter as compared to Topex-A altimeter. This difference may be caused by several factors. The first one being that both altimeters sampled the jet over different periods and when averaged over the sampling period, the climatologies will exhibit variations in both current strength and position. Another reason for the differences observed in the Jason and Topex climatologies is that the raw observations SSH made from Jason-1 are made at different frequencies (20Hz for Jason-1 and 10Hz for Topex) (Gille, 2004). The seaward edge of the Benguela Jet could be observed near the 500 m isobath throughout the year in the altimeters observations collected along the J1_31 and Tp_31 tracks. While the jet exists throughout the year; the location of its dynamical core varies seasonally. However J1_31 and Tp_31 failed to

capture the Benguela Jet close to the coast due to signal contamination near the shore (Rouault *et al*., 2010).

The altimetry and model both revealed a region of increased current flow associated with the presence of Benguela Jet. The position of the jet in altimetry and the model are in agreement with the SST climatology which suggests that the jet is an upwelling jet, driven by changes in SST and SSH associated with presence of colder waters near the coast due to coastal upwelling. This is similar to other upwelling jets in the Iberian, Californian and Central Chilean current systems that occur between colder upwelled waters and warmer oceanic waters (Peliz *et al*., 2002; Barth *et al*., 2000; Mesias *et al*., 2001).

The existence of the Benguela Jet off Cape Columbine and the Cape Peninsula observed in the model and satellite data is consistent with the finding of Boyd *et al*., (1992). The speed of the jet estimated from the geostrophic derived currents of both the model and satellite altimeter data is within the range of 0.5-0.8 $m.s^{-1}$ observed by Strub *et al*., (1998) and Huggett *et al*., (1998). These current speeds are of the same order of magnitude as in other upwelling Jets studied around the world, with the velocities of the equatorward jet off northern California observed by Strub and James (2000) ranging from 0.5-0.7 $m.s^{-1}$ and the equatorward jet in the Iberian system has a speed of about 0.4 $m.s^{-1}$ (Peliz *et al*., 2002).

2.4.2 Annual Cycle

The model and satellite data showed distinct annual variations in the Benguela Jet properties, with different intensities and position of the jet in austral summer and winter.

The model data reproduced the existence of the Benguela Jet in the southern Benguela region. The total surface and geostrophic currents derived from the model showed a strong seasonal signal of the jet. The jet current was narrow and strong in January (austral summer) with velocities of 0.6-0.75 $m.s^{-1}$, which can be associated to intense upwelling at the peak of the austral summer season and forcing by the wind stress curl. The jet also migrated farther offshore due to persistent upwelling and offshore displacement of thermal front associated with upwelling cells (Huggett *et al*., 1998). During summer, upwelling lowers the steric height and an increase of the steric heights due to intrusion of Agulhas Current waters at the seaward boundary of the Benguela Jet results into the intensification of the jet (Strub *et al*., 1998). The results from the model also resolved the jet extending from Cape Agulhas to Cape

Columbine in January during the summer upwelling season. This is consistent with the findings of Veitch *et al*., (2009). The jet separated into a strong offshore component and a coastal component off the Cape Columbine, consistent with the findings of Boyd and Nelson (1998). The detachment of the Benguela Jet from the coast off the Cape Columbine is similar to that observed in the equatorward jet that separates from the coast south off Oregon and off Punta Lavapie (Barth *et al*., 2000; Aguirre *et al*., 2012). The model jet broadened and weakened in July (0.4-0.5 $m.s^{-1}$) probably due to relaxation of upwelling favourable winds during austral winter. During July the jet was confined to the coast and was stronger off Cape Peninsula (0.5 $m.s^{-1}$) as compared to the Cape Columbine (0.4 $m.s^{-1}$) due to the locality of warm Agulhas waters with high steric height (Strub *et al*., 1998). The velocities of the jet in winter of 0.5 $m.s^{-1}$ off Cape Peninsula is in agreement with the findings of Butler (2012). The strengthening of the Benguela Jet in summer and the weakening in winter observed in the model is similar to other upwelling jets that have been documented in the Californian, Iberian and Central Chilean systems (by Strub & James, 2000; Peliz *et al*., 2002; Mesias *et al*., 2002).

The altimeter data was able to capture the characteristics of the jet along the west coast. Across-track geostrophic velocities derived from J1_209 and Tp_209 altimeter tracks were able to highlight the lateral displacement of the jet in January and showed that it shifted farther offshore due to prolonged upwelling associated with the Cape Columbine upwelling cell. The jet was weaker and closer to the shore in July. The jet as observed in the Topex-A altimetry dataset appeared stronger than in Jason-1A altimetry dataset in both January and July. This may be due to the different averaging periods used when computing the climatologies of across-track velocities to characterize the Benguela Jet. The Topex-A spans 11 years (1992-2002) while Jason1A spans 8 years (2002-2009). Hence there may be an influence of interannual variability in the climatologies created. The other reason could be due to the sampling capabilities of Jason1, which are an improvement on Topex-A (Gille, 2004). The J1_31 and Tp_31 tracks only captured the seaward edge of the jet in January and could not adequately resolve the jet in July when it was closer to the coast. This is due to the fact that the altimeter data is contaminated close to the coast by land interference and other problems such as the large foot print of on-board radiometers which are used for wet tropospheric corrections (Rouault *et al*., 2010). SSH observations from altimeters are also limited near the shore due to the inability of altimeters to resolve high frequencies SSH variability caused by barometric fluctuations or non-linear interactions of the tides with the

topography (Rouault *et al*., 2011). Therefore there is no data along these tracks within 50 km from the coast which makes it difficult to note the presence of the jet. Strub *et al*., (1998) could also only resolve the offshore part of the jet using two years of Goesat altimetry data.

Regions of intensified flow are often associated with strong SSH and SST gradients (Strub *et al.,* 1998). The inshore boundary of the Benguela Jet has been observed to coincide with a strong temperature front, which separates the upwelling coastal regions from the warmer offshore regions (van der Lingen and Huggett, 2003). In Section three of this thesis, regions of strong SST and SSH gradient were computed in an attempt to identify the Benguela Jet. In the SST and SSH, the strongest gradients were encountered between 17.4-17.6^{o}E based on Jason1A and between 17.5-17.6^{o}E based on Topex-A off Cape Columbine in January. The different positions observed in the two altimetry missions could be due to variations in the Jet properties during the time periods sampled by each mission as the missions follow each other across the Benguela Jet region. Weaker gradients were encountered at the same positions in July, this is due to the inability of the altimeter to resolve the natural migration of the jet as the jet separates into an offshore and inshore component. The jet resolved by satellite altimeters also varied between the 200 m and 500 m isobaths as documented by (van der Lingen & Huggett 2003; Fowler & Boyd, 1998). The thermal front was stronger and farther offshore in January due to active upwelling and pushed the jet farther offshore. While in July the front was weak and close to the coast. The position and strength of the jet is related to the seasonal variation of the thermal front (Bang & Andrews, 1974).

The seasonal signal was strongly pronounced in the model data as compared to the satellite altimeter due to the fact that the model is forced with 0.5^{o} QuikSCAT monthly climatological wind (Veitch, 2009) as the jet is predominantly driven by the wind stress. A time-series of cross-track geostrophic velocities was computed for each altimeter mission in order to verify if there were seasonal signals within each year. The altimeter data showed interannual variability of the jet and a generally weak seasonal cycle. This explains the poorly defined seasonal cycle in the climatology derived from the altimetry datasets.

Chapter 3: Conclusion

The Benguela Jet has been the subject of numerous biological studies which aimed to resolve transport pathways of fish eggs and larvae from the spawning grounds of the Agulhas Bank to the nursery areas of the Benguela upwelling ecosystem. The dynamics of the jet which drives the transport of fish and egg larvae from the west to the east coast of South Africa remain poorly understood. The objective of this study was to investigate the annual cycle of the Benguela Jet. In this chapter we summarise the findings based on the questions underlined in Chapter two, Section one and which are as follows:

1. Can the Jet be identified in altimeter and SST satellite data?

The altimeter and SST satellite data resolved the existence of the jet off the Cape Peninsula and Cape Columbine. In the SST and SSH gradients the dynamical core of the Benguela Jet was located between 17.4-17.6^{o}E in both Jason-1A and Topex-A off the Cape Columbine. In the J1_31 and Tp_31 track altimetry datasets, the position of the jet was between 18-18.2^{o}E in January off Cape Peninsula. The geostrophic currents derived from all altimeter missions resolved the presence of the Benguela Jet off the Cape Peninsula and Cape Columbine. Along tracks and in the southern section of the Bengulea Jet, a large portion of the altimetry data was flagged closer to the coast due to land contamination and the large footprint of the on-board radiometers. This resulted in the Benguela Jet not being adequately captured within the altimetry datasets.

2. How well does the jet in the satellite data compare to the model?

The satellite and the model both resolved the existence of the Benguela Jet in the southern Benguela region. The core of the jet was stronger off the Cape Peninsula in both geostrophic currents (0.6 m.s^{-1}) and surface currents (0.7 m.s^{-1}) derived from the model. The model resolved the jet extending from Cape Agulhas to Cape Columbine, unlike the altimetry. The speed of the jet estimated from both the geostrophic derived model and satellite altimeter data was within the range of 0.5-0.8 m.s^{-1}, in agreement with previous studies. This shows the ability of the satellite data to capture the main features of the jet. Although the presence of southward flow over the study region falls beyond the scope of this study it is worth mentioning that strong southward currents were observed in the altimetry but not in the model data.

3. What is the annual cycle of the jet (both position and strength)?

January and July months represented the austral summer and winter months. The seasonal characteristics of the jet are similar between the altimeter and model datasets except that the seasonal variation of the jet was strongly pronounced in the model. The model and altimeter data especially the J1_209 and Tp_209 tracks resolved the seasonal patterns of the Benguela Jet. The jet was narrow and strong in January reaching speeds up to 0.6 $m.s^{-1}$ off Cape Columbine and 0.75 $m.s^{-1}$ off the Cape Peninsula and was situated farther offshore based in the model, relative to the altimeter data. Outputs from the numerical model showed that in July the jet was confined to the coast and was stronger off the Cape Peninsula (0.5 $m.s^{-1}$) than off Cape Columbine (0.4 $m.s^{-1}$). J1_209 and Tp_209 tracks also resolved a strong jet off Cape Columbine in January. Whereas the altimetry dataset for J1_31 and Tp_31 tracks only reproduced the strong jet in January and failed to resolve the jet in July. The altimeter data showed interannual variability of the jet. This concludes that the Benguela Jet is stronger in summer and weaker in winter.

The altimetry data was both temporally and spatially limited which made it difficult to observe seasonal signal of the jet especially when it was closest to the coast and other limiting factor is that the jet is small in dimension. Therefore the recommendation for future studies of the Benguela Jet current would be to use the highest resolution altimeter data available and to use coastal altimetry products so that the tracks can resolve the jet especially off the Cape Peninsula. High resolution altimeter data with longer time series may be necessary to investigate the seasonal patterns of the Benguela Jet. An in-depth understanding of the Benguela Jet's annual cycle would be gained through the use of higher resolution models and in situ data. It would be beneficial to investigate a higher resolution model, as well as one forced by higher resolution (both temporally and spatially) winds. Some idealized model studies would help answer specific questions around the jet, such as by shutting off the Agulhas Current input.

References

Aguirre, C., Pizarro, Ó., Strub, P. T., Garreaud, R. and Barth, J. A. (2012). Seasonal dynamics of the near-surface alongshore flow off central Chile. *Journal of Geophysical Research* , **117**, C01006, doi:10.1029/2011JC007379.

Ambar, I. and Fiúza, A.F.G. (1994). Some features of the Portugal current system: A poleward slope undercurrent, an upwelling related summer southward flow and autumn-winter poleward coastal surface current, in *proceedings of the 2nd* International Conference on Air-Sea Interaction, Meteorology and Oceanography of *the Coastal Zone*, edited by K.Katsaros, A. Fiúza and I.Ambar, p311, American Meteorology Society

Bakun, A. and Nelson, C. S. (1991). The seasonal cycle of wind-stress curl in subtropical eastern boundary current regions. *Journal of Physical Oceanography*, **21**: 1815-1834.

Bang, N. D. and Andrews, W. R. H. (1974). Direct current measurement of a shelf-edge frontal jet in the southern Benguela system. *Journal of Marine Science.* **32** (3), pp. 405-417.

Barth, J. A. and Smith, R. L. (1998). Separation of a coastal upwelling jet at Cape Blanco, Oregon, USA. In: Pillar, S. C., Moloney, C. L., Payne, A. I. L., Shillington, F. A. (Eds.), Benguela Dynamics: Impacts of Variability on Shelf-Sea Environments and their Living Resources. *South African Journal of Marine Science*, **19**: 5-14.

Barth, J. A., Pierce, S. D. and Smith, R. L. (2000). A separating coastal upwelling jet at Cape Blanco, Oregon and its connection to the California Current System. *Deep-Sea Research II*, **47**: 783-810.

Barth, J. A., Pierce, S. D. and Cowles, T. J. (2005). Mesoscale structure and its seasonal evolution in the northern California Current System. *Dee-Sea Research II*, **52**: 5-28.

Blanke, B., Penven, P., Roy, C. and Chang, N. (2009). Ocean variation over the Agulhas Bank and its dynamics connection with the southern Benguela upwelling system. *Journal of Geophysical Research*, **114**, C12028, doi: 10299/2009JC005358.

Boyd, A. J., Taunton-Clark, J. and Oberholster, G. P. J. (1992). Spatial features of the near-surface and midwater circulation patterns off western and southern South Africa and their role in the life histories of various commercially fished species. *South African Journal of Marine Science*, **12** (1): 189-206.

Boyd, A. J. and Nelson, G. (1998). Variability of the Benguela Current off the Cape Peninsula, South Africa. *South African Journal of Marine Science*, **19** (1): 27-29.

Butler J. (2012). Near-surface hydrography in the region of the Good Hope Jet from 4 years of cruise data. Honours thesis, University of Cape Town, Rondebosch, South Africa.

Dufois, F. and Rouault, M. (2012). Sea Surface temperature in False Bay (South Africa): Towards a better understanding of its seasonal and inter-annual variability. *Continental Shelf Research*, **43**: 24-35.

Dufois, F., Penven, P., Whittle, C. and Veitch, J. (2012). On the warm nearshore bias in Pathfinder monthly SST products over Eastern Boundary Upwelling Systems. Ocean *Modelling*, **47**: 113-118.

Fawcett, A. L., Pitcher, G.C. and Shillington, F.A. (2008). Nearshore currents on the southern Namaqua shelf of the Benguela upwelling system. *Continental Shelf Research*, **28**: 1026-1039.

Fowler, J. L. and Boyd, A. J. (1998). Transport of anchovy and sardine eggs and larvae from the western Agulhas Bank to the West Coast during the 1993/94 and 1994/95 spawning seasons. *South African Journal of Marine Science*, **19**: 181-195.

Gille, S. T. (2004). Using Kolmogorov-Smirnov statistics to assess Jason, TOPEX and Poseidon altimeter measurements. *Marine Geodesy,* **27**: 47-58.

Grote, B., Ekau, W., Hagen, W., Huggett, J. A. and Verheye, H. M. (2007). Early life-history strategy of Cape hake in the Benguela upwelling region. *Fisheries Research*. **86**: 179-187.

Hardman-Mountford, N. J., Richardson, A. J., Agenbag, J. J., Hagen, E., Nykjaer, L., Shillington, F. A., and Villacastin, C. (2003). Ocean climate of the South East Atlantic observed from satellite data and wind models. *Progress in Oceanography,* **59:** 181–221.

Huggett, J., Fréon, P., Mullon, C. and Penven, P. (2003). Modelling the transport success of anchovy Engraulis encrasicolus eggs and larvae in the Southern Benguela: the effect of spatio-temporal spawning patterns. *Marine Ecology Progress Series.* **250**: 247-262.

Huggett, J. A., Boyd, A. J., Hutchings, L. and Kemp, A. D. (1998). Weekly variability of clupeoid eggs and larvae in the Benguela jet current: implications for recruitment. *South African Journal of Marine Science*, **19** (1): 197-210.

Hutchings, L. (1992). Fish harvesting in a variable, productive environment-searching for rules or searching for execeptions?, *South African Journal of Marine Science*, **12** (1): 297-318.

Hutchings, L., Barange, M., Bloomer, S. F., Boyd, A. J., Crawford, R. J. M., Huggett, J. A., Kerstan, M., Korrubel, J. L., De Oliveira, J. A. A., Painting, S. J., Richardson, A. J., Shannon, L. J., Schulein, F. H., van der Lingen, C. D. and Verheye, H. M. (1998). Multiple factors affecting South African anchovy recruitment in the spawning, transport and nursery areas. *South African Journal of Marine Science*, **19**: 211-225.

Hutchings, L. and Boyd, A. J. (1992). Environmental influences on the purse seine fishery in South Africa. *Investigación Pesq*., Santiago, 37: 23–43.

Huyer, A., Kosro, M. P., Fleischbein, J., Ramp, S. R., Stanton, T., Washerburn, L., Chavez, F. P., Cowles, T. J., Pierce, S. D. and Smith, R. L. (1991). Currents and Water Masses of the Coastal Transition Zone off Northern California, June to August 1988. *Journal of Geophysical Research*, **96** (8): 14,809-14,831.

Krug, M. and Tournade, J. (2012). Satellite observations of an annual cycle in the Agulhas Current. *Geophysical Research Letters*, **39** (15): L15607, doi: 10.1029/2012GL052335.

Lutjeharms, J. R. E. (1981) Satellite studies of the South Atlantic upwelling system. *In Oceanography from Space.* Gower, J. F. R. (Ed.). New York; Plenum: 195-199.

McMurray, H. F., Carter, R. A. and Lucas, M. I. (1993). Size-fractionated phytoplankton production in western Agulhas Bank continental shelf waters. *Continental Shelf Research*, **13** (2/3): 307-329.

Merchant, C. J., Le Borgne, P., Roquet, H. and Marsouin, A. (2009). Sea surface temperature from a geostationary satellite by optimal estimation. *Remote Sensing of Environment*, **113**: 445-457.

Mesias, J., Matano, R. and Strub, P. T. (2001). A numerical study of the upwelling circulation off central Chile. . *Journal of Geophysical Research,* **106***:* 19611-19623, doi:10.1029/2000JC000649.

Mesias, J., Matano, R. and Strub, P.T. (2003), Dynamical analysis of the upwelling circulation off central Chile. *Journal of Geophysical Research,* **108**: 3085, doi:10.1029/2001JC001135.

Minnett, J. P., Evans, R. H., Kearns, E. J. and Brown, O. B. (2002). Sea surface temperature measured by the Moderate Resolution Imaging Spectroradiometer (MODIS). *In: International Geosciences and Remote Sensing Symposium*, Toronto, Canada, June 24–28, 2002.

Mullon, C. Freon, P., Parada, C., van der Lingen, C. and Huggett, J. (2003). From particles to individuals: modelling the early stages of anchovy *(Engraulis capensis*/*encrasicolus*) in the southern Benguela. *Fisheries Oceanography,* **12**: 396-406.

Nelson, G. and Hutchings, L. (1983). The Benguela upwelling area. *Progress in Oceanography,* **12** (3): 333-356.

Nelson, G. (1989). *Poleward Flows along eastern ocean boundaries,* Coastal and Estuarine Studies, **34**. Poleward motion in the Benguela area, 110-130, Springer: New York.

Nicholson, S. E. (2010). A low-level jet along the Benguela coast, an integral part of the Benguela current ecosystem. *Climatic Change,* **99**: 613-624.

Penven, P., Roy, C., Brundrit, G., Verdiere, A. D., Freon, P., Johnson, A., Lutjeharms, J. and Shillington, F. (2001). A regional hydrodynamic model of upwelling in the southern Benguela. *South African Journal of Science*, **97:** 472-475.

Peliz, A., Rosa, T. L., Santos, M. A. and Pissarra. (2002). Fronts, jets and counter-flows in the Western Iberian upwelling system. *Journal of Marine Systems*, **35;** 67-77.

Pitcher, G. C., Bernard, S. and Ntuli, J. (2008). Constrasting Bays and red tides in the Southern Benguela Upwelling System. *Oceanography*, **21** (3): 82-91.

Preston-Whyte, R. and Tyson, P. (1993). *The atmosphere and weather of southern Africa*, Chapter. 11, 209-249. Oxford.

Relvas, P. and Barton, E. D. (2005). A separate jet and coastal counterflow during upwelling relaxation off Cape São Vicente (Iberian Peninsula).*Continental Shelf Research*, **25**: 29-49.

Rio, M. H. S. G. and Larnicol, G. (2011). The CNES-CLS09 global Mean Dynamic Topography computed from the combination of GRACE data. Altimetry and in-situ measurements. *Journal of Geophysical Research,* **116,** C07018, doi: 10.1029/201JC006505.

Robinson, I. S. (2010). *Discovering the ocean from space*: The unique application of satellite oceanography. Chichester, UK: Springer Praxis Publishing.

Rouault, M. (2011). Agulhas Current variability determined from space: A multi-sensor approach. PhD thesis, University of Cape Town, Rondebosch, South Africa.

Rouault, M. J., Mouche, A., Collard, F., Johannessen, J. A. and Chapron, B. (2010). Mapping the Agulhas Current from space: An assessment of ASAR surface current velocities. . *Journal of Geophysical Research,* **115**: C10026, doi: 10.1029/2009JC006050.

Sánchez, R. F. and Relvas, P. (2003). Spring-summer climatological circulation in the upper layer in the region of Cape St. Vincent, Southwest Portugal. *Journal of Marine Science*, **60**: 1232-1250.

Schrama, E., Scharroo, R. and Naeije, M. (2000). Radar Altimeter Database System (RADS): Towards a generic multi-satellite altimeter database system, Final Report.,88p., *SRON/BCRS publ., USP-2 report 00-11, ISBN 90-54-11-319-7* September 2000.

Shchepetkin, A. F., and McWilliams, J. C. (2005). The Regional Oceanic Modeling System (ROMS): A split-explicit, free-surface, topography following-coordinate oceanic model. *Ocean Modelling*, **9** (4): 347–404.

Shannon, L. V. and Nelson, G. (1996). The Benguela: Large-scale features and processes and system variability. The South Atlantic: Present and Past Circulation, G. Wefer, Ed., Springer, 163–210.

Shelton, P. A., Hutchings, L., 1982. Transport of anchovy, *Engraulis capensis* Gilchrist, eggs and early larvae by a frontal jet current. *ICES Journal of Marine Science,* **40** (2): 185–198.

Shillington, F. A., Reason, C. J. C., Duncombe-Rae, C. M., Florenchie, P. and Penven, P. (2006). *Benguela: predicting a large marine ecosystem,* Large Marine Ecosystems, **14**, Chapter 4: Large scale variability of the Benguela Current Large Marine Ecosystem (BCLME), 49–70. Elsevier B.V.

Shillington, F. A. (1998). The Benguela upwelling system off southwestern Africa. *The Sea,* **11**: 583-604.

Strub, P., Shillington, F., James, C. and Weeks, S. (1998). Satellite comparison of the seasonal circulation in the Benguela and California current systems. *South African Journal of Marine Science*. **19**: 99-112.

Strub, P. T. and James, C. (1995). The large-scale summer circulation of the California current. *Geophysical Research Letters,* **22** (3): 207-210.

Strub, P. T., James, C. (2000). Altimeter-derived variability of surface velocities in the California Current System: 2. Seasonal circulation and eddy statistics. *Deep-Sea Research Part II,* **47**: 831–870.

van der Lingen, C. D. and Huggett, J. A. (2003). The role of ichthyoplankton surveys in recruitment research and management of South African anchovy and sardine. In: H. I. Browman and A. B. Skiftesvik, ed. 2003. *The Big Fish Bang.* Norway: Institute of Marine Research, 303-343.

Veitch, J. (2009). Equilibrium dynamics of the Benguela system: A numerical modelling approach. PhD thesis, University of Cape Town, Rondebosch, South Africa.

Veitch, J., Penven, P., and Shillington, F. (2009). The Benguela: A laboratory for comparative modeling studies. *Progress in Oceanography*, **83**: 296-302.

Veitch, J., Penven, P., and Shillington, F. (2010). Modeling Equilibrium Dynamics of the Benguela Current System. *Journal of Physical Oceanography,* **40**: 1942-1964.

Weeks, S. J., Barlow, R., Roy, C. and Shillington, F. A. (2006). Remotely sensed variability of temperature and chlorophyll in the southern Benguela: Upwelling frequency and phytoplankton response. African Journal of Marine Science, **28**: 493–509.